Supporting information for:
"Mini-β-barrels From Short Macrocyclic Peptides"

Viet Thuc Dang[a], Michael W. Martynowycz[b,c], Dan McElheny[a], Andy I. Nguyen*[a]

[a] Department of Chemistry, University of Illinois Chicago, Chicago, Illinois 60607, United States

[b] UB Hauptman-Woodward Institute (UB-HWI), University at Buffalo, Buffalo, NY 14203, United States

[c] Department of Structural Biology, Jacobs School of Medicine and Biomedical Sciences, University at Buffalo, Buffalo, NY 14203

*Corresponding author. *E-mail*: andyn@uic.edu

Table of Contents

I. General considerations

Trifluoroacetic acid (TFA), triisopropylsilane (TIPS), *N*,*N*'-diisopropylcarbodiimide (DIC), Fmoc-L-Trp(Boc)-OH, Fmoc-His(Trt)-OH, Fmoc-L-Ser(tBu)-OH, Fmoc-L-Phe-OH, Fmoc-L-Ile-OH, Fmoc-Sar-OH, Fmoc-N-methyl-Ala-OH, *N*α-Boc-*N*δ-Fmoc-L-Orn-OH, Fmoc-L-His(π-Me)-OH, ethyl(hydroxyimino) cyanoacetate (Oxyma), *N*,*N*-diisopropylethylamine (DIPEA), (1-cyano-2-ethoxy-2oxoethylidenaminooxy)dimethylamino-morpholino-carbenium hexafluorophosphate (COMU), and 2-chlorotrityl chloride resin were purchased from Chem-Impex International Inc. Acetonitrile (MeCN) was purchased from Millipore Sigma. Dichloromethane (DCM) and 4-methyl-piperidine were purchased from Fisher. *N*, *N*-dimethylformamide (DMF), 4-(2-hydroxyethyl)-1-piperazineethanesulfonic acid (HEPES), and 2,3,4-trimethylpyridine (collidine) was purchased from Sigma-Aldrich.

II. Synthesis and characterization

Structure of reported peptides

Synthesized peptides were exposed to trifluoroacetic acid during the purification process. Masses used for the preparation of samples from lyophilized solid peptide account for the presence of these trifluoroacetate counterions based on the number of functional groups with pK_a values greater than that of trifluoroacetic acid. The adjusted mass and expected number of counterions are given below each structure.

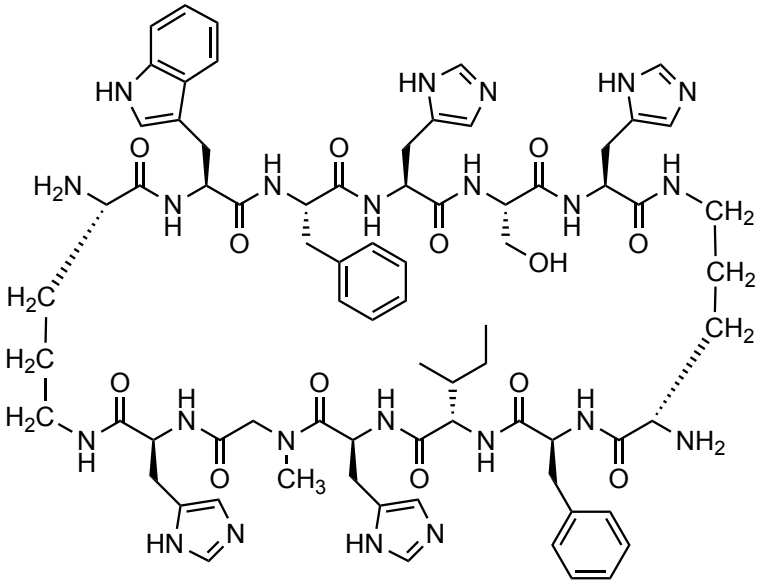

MC4H

MW: 1528.75
MW+6TFA: 2212.89

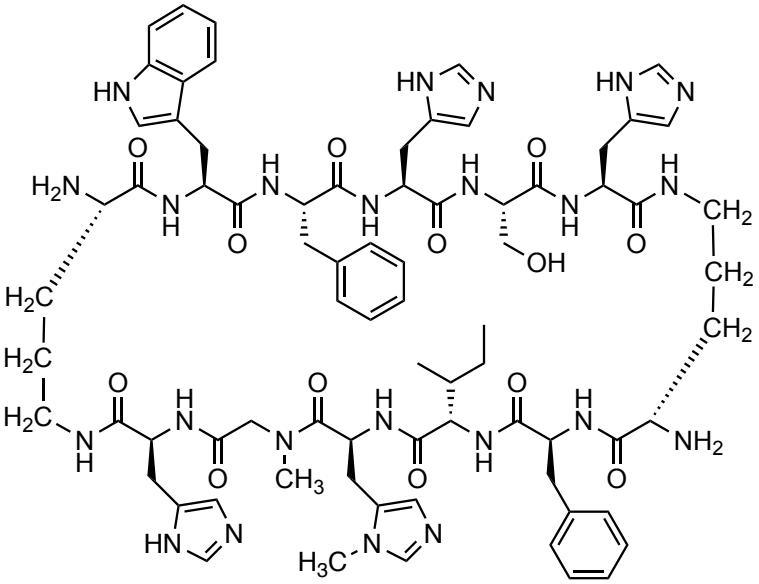

MC4H-MeH

MW: 1542.78
MW+6TFA: 2226.92

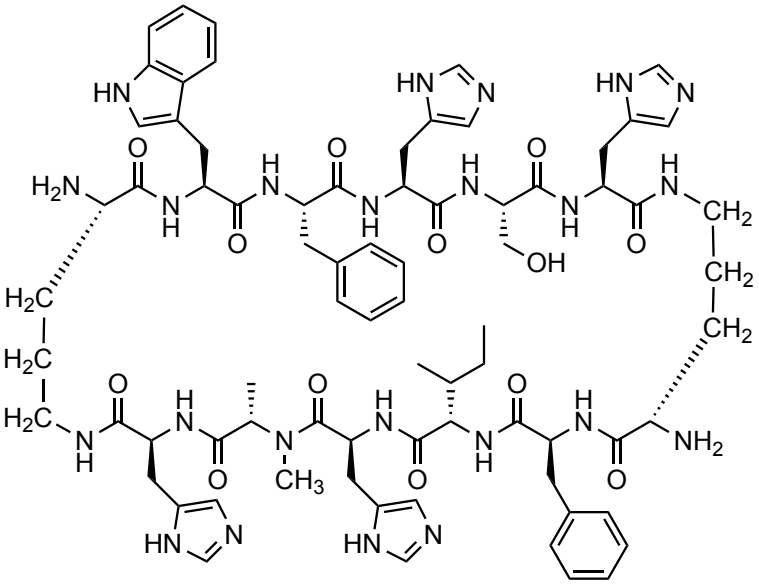

MC4H-MeA

MW: 1542.78
MW+6TFA: 2226.92

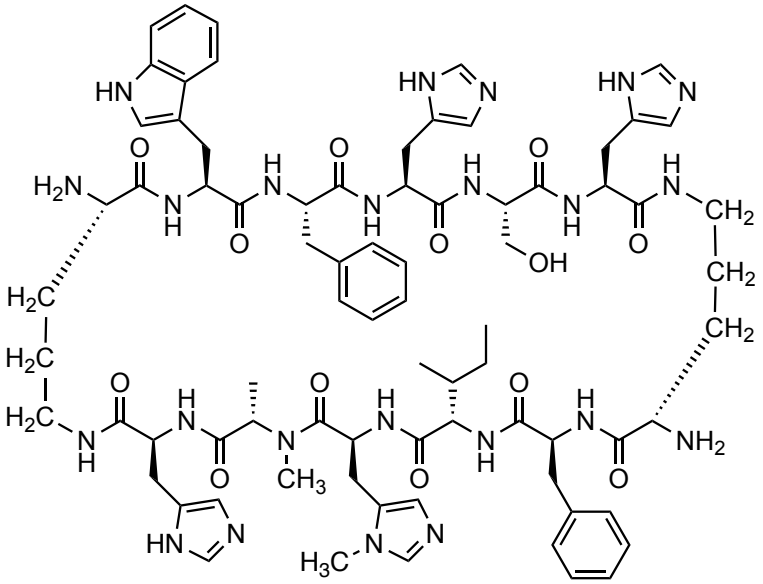

MC4H-MeAMeH

MW: 1556.80
MW+6TFA: 2240.94

Resin loading determination

2-chlorotrityl chloride resin was coupled with Fmoc-Trp(Boc)-OH, and the resin loading was determined by the amount of attached Fmoc released during deprotection by 4-methylpiperidine.

A ~0.1 mmol of 2-chlorotrityl chloride resin (based on the loading reported by the manufacturer) was allowed to swell in 5 mL DCM at room temperature while being agitated with N_2 gas for 10 min, and then it was drained. 0.22 mmol of Fmoc-Trp(Boc)-OH was dissolved in 8 mL of DCM and 0.3 mL of 2,4,6-collidine, and this mixture was added into the swelled 2-chlorotrityl chloride resin and agitated on an orbital shaker for 8 hr at room temperature, and then it was drained. The resin was initially washed 4 times, each by adding 5 mL DCM, agitating with N_2 for 5 s, and then drained under vacuum. The resin was thoroughly air-dried by pulling vacuum through the cartridge for 30 min.

A known amount of dried resin was transferred into a 1.5 mL microcentrifuge tube, and DMF (800 µL) was added and allowed to swell for 15 mins. Then, 4-methylpiperidine (200 µL) was added, and the mixture was allowed to stand at room temperature for 15 min. The solution above the resin (100 µL) was transferred to a 1 cm quartz cuvette and diluted with DMF (900 µL). A UV-vis spectrum was recorded. The absorbance at 301 nm was used to calculate the resin loading (eq 1). The average resin loading acquired from the four measurements was 0.34 mmol/g.

$$L = \frac{(A_{301} \times V \times d)}{(\varepsilon \times w \times M)} \qquad \text{(eq S1)}$$

where L = resin loading (mmol/g)
A_{301} = absorbance at 301 nm
V = volume of sample (mL)
d = dilution factor = 10
ε = extinction coefficient of Fmoc = 7800 (mL $mmol^{-1}cm^{-1}$)
w = path length of cuvette (cm)
M = mass of resin used (g)

Preparation of amino acid solution

For a 0.1 mmol scale, 0.20 M of amino acid in DMF is used. 2.5 mL of this solution is used for each coupling step.

Preparation of Oxyma Pure (ethyl cyano(hydroxyimino)acetate) solution

For a 0.1 mmol scale, 1 M of Oxyma Pure in DMF is used. 0.5 mL of this solution is used for each coupling step.

Preparation of DIC (N,N'-Diisopropylcarbodiimide) solution

For a 0.1 mmol scale, 1 M of DIC in DMF is used. 1.0 mL of this solution is used for each coupling step.

Preparation of 4-methylpiperidine solution

For a 0.1 mmol scale, 20% v/v concentration of 4-methylpiperidine in DMF is used. 2.0 mL of this solution is used for each coupling step.

Scheme for automated synthesis

Peptides were synthesized on a 0.1 mmol scale using the CEM Liberty Blue automated peptide synthesizer. The solvent for all SPPS solutions was DMF unless otherwise stated. The prepared amino acid, Oxyma, and DIC concentrations were 0.20 M, 1.0 M, and 1.0 M respectively. The deprotection solution was 20% (v/v) 4-methylpiperidine in DMF.

1. ***Swelling:*** 2-chlorotrityl resin preloaded with Fmoc-Trp(Boc)-OH (see "Resin Loading Determination" section above) was allowed to swell in 5 mL DMF at room temperature while being agitated with N_2 gas for 10 min, and then it was drained.

2. ***Single coupling 0.1 mmol scale:*** A 2 mL volume of 4-methyl-piperidine in DMF (20% v/v) was added to the swelled resin and agitated with N_2 gas for 15 s at 90° C, and then it was drained. The resin was washed 4 times, each by adding 5 mL DMF, agitating with N_2 for 5 s, and then drained. 1.0 mL of 1.0 M DIC and 0.5 mL of 1.0 M Oxyma was added to the reaction vessel containing the resin followed by 2.5 mL of 0.20 M amino acid solution. The solution was allowed to warm to75° C over the course of 15s and followed by and interval of 110 s being held at 90° C. N2 gas was used to agitate the reaction vessel before being drained. The resin was washed 4 times, each by adding 5 mL DMF, agitating with N_2 for 5 s, and drained.

3. ***Double histidine coupling 0.1 mmol scale:*** A 2 mL volume of 4-methyl-piperidine in DMF (20% v/v) was added to the swelled resin and agitated with N_2 gas for 15 s at 90° C, and then it was drained. The resin was washed 4 times each by adding 5 mL DMF, agitating with N_2 for 5 s, and drained. A volume of 1.0 mL of 1.0 M DIC and 0.5 mL of 1.0 M Oxyma was added to the reaction

vessel followed by a volume of 2.5 mL of 0.20 M Fmoc-His(Trt)-OH solution. The solution was ramped to 50 °C over 120 s followed by 480 s held at 50° C with N_2 gas agitation, the reaction vessel was drained. Another round of Oxyma, DIC, and Fmoc-His(Trt)-OH were added as previously described. The resin was washed 4 times, each by adding 5 mL DMF, agitating with N_2 for 5 s, and drained.

4. ***Manual π-methyl histidine coupling 0.1 mmol scale:*** Due to the insolubility of Fmoc-His(π-Me)-OH in DMF, this residue was coupled on manually. The Fmoc-deprotected resin-bound peptide was transferred to a fritted jacketed reaction column using DMF to as a medium. The DMF was drained from the reaction column and the resin was washed 4 times each by adding 5 mL DMF. A 4 mL activated amino acid mixture was made by mixing 2.5 mL of 0.20 M Fmoc-His(π-Me)-OH, 1.0 mL of 0.45 M COMU, and 0.5 mL of 1.6 M DIPEA and was added to the resin. The reaction was allowed to proceed for 35 mins at 50 °C with N_2 gas agitation, and then the reaction column was drained. The resin was washed 4 times with 5 mL DMF and later returned to the CEM Liberty Blue. This procedure is only used for the synthesis of **MC4H-MeH** and **MC4H-MeAMeH**.

5. ***Final deprotection:*** The N-terminal amino acid was deprotected with 4 mL of 20% (v/v) 4-methyl-piperidine for 50 s then drained. The resin was then washed 4 times with 4 mL of DMF and drained.

Table S1. MC4H

Step	Amino Acid	Specific A.A. Derivative	Cycle
1	Trp	Fmoc-Trp(Boc)-OH	swelling (preloaded resin)
2	Orn	Boc-Orn(Fmoc)-OH	single coupling
3	His	Fmoc-His(Trt)-OH	double histidine coupling
4	Sar	Fmoc-Sar-OH	single coupling
5	His	Fmoc-His(Trt)-OH	double histidine coupling
6	Ile	Fmoc-Ile-OH	single coupling
7	Phe	Fmoc-Phe-OH	single coupling
8	Orn	Boc-Orn(Fmoc)-OH	single coupling
9	His	Fmoc-His(Trt)-OH	double histidine coupling
10	Ser	Fmoc-Ser(tBu)-OH	single coupling
11	His	Fmoc-His(Trt)-OH	double histidine coupling
12	Phe	Fmoc-Phe-OH	single coupling
13	N/A	N/A	final deprotection

Table S2. MC4H-MeH

Step	Amino Acid	Specific A.A. Derivative	Cycle
1	Trp	Fmoc-Trp(Boc)-OH	swelling (preloaded resin)
2	Orn	Boc-Orn(Fmoc)-OH	single coupling
3	His	Fmoc-His(Trt)-OH	double histidine coupling
4	Sar	Fmoc-Sar-OH	single coupling
5	N/A	N/A	final deprotection
		Removed from CEM for manual coupling of MeH residue	
6	MeH	Fmoc-His(π-Me)-OH	Swelling (preloaded resin)
7	Ile	Fmoc-Ile-OH	single coupling
8	Phe	Fmoc-Phe-OH	single coupling
9	Orn	Boc-Orn(Fmoc)-OH	single coupling
10	His	Fmoc-His(Trt)-OH	double histidine coupling
11	Ser	Fmoc-Ser(tBu)-OH	single coupling
12	His	Fmoc-His(Trt)-OH	double histidine coupling
13	Phe	Fmoc-Phe-OH	single coupling
14	N/A	N/A	final deprotection

Table S3. MC4H-MeA

Step	Amino Acid	Specific A.A. Derivative	Cycle
1	Trp	Fmoc-Trp(Boc)-OH	Swelling (preloaded resin)
2	Orn	Boc-Orn(Fmoc)-OH	single coupling
3	His	Fmoc-His(Trt)-OH	double histidine coupling
4	MeA	Fmoc-N-Me-Ala-OH	single coupling
5	His	Fmoc-His(Trt)-OH	double histidine coupling
6	Ile	Fmoc-Ile-OH	single coupling
7	Phe	Fmoc-Phe-OH	single coupling
8	Orn	Boc-Orn(Fmoc)-OH	single coupling
9	His	Fmoc-His(Trt)-OH	double histidine coupling
10	Ser	Fmoc-Ser(tBu)-OH	single coupling
11	His	Fmoc-His(Trt)-OH	double histidine coupling
12	Phe	Fmoc-Phe-OH	single coupling
13	N/A	N/A	final deprotection

Table S4. MC4H-MeAMeH

Step	Amino Acid	Specific A.A. Derivative	Cycle
1	Trp	Fmoc-Trp(Boc)-OH	Swelling (preloaded resin)
2	Orn	Boc-Orn(Fmoc)-OH	single coupling
3	His	Fmoc-His(Trt)-OH	double histidine coupling
4	MeA	Fmoc-N-Me-Ala-OH	single coupling
5	N/A	N/A	final deprotection
		Removed from CEM for manual coupling of MeH residue	
6	MeH	Fmoc-His(π-Me)-OH	Swelling (preloaded resin)
7	Ile	Fmoc-Ile-OH	single coupling
8	Phe	Fmoc-Phe-OH	single coupling
9	Orn	Boc-Orn(Fmoc)-OH	single coupling
10	His	Fmoc-His(Trt)-OH	double histidine coupling
11	Ser	Fmoc-Ser(tBu)-OH	single coupling
12	His	Fmoc-His(Trt)-OH	double histidine coupling
13	Phe	Fmoc-Phe-OH	single coupling
14	N/A	N/A	final deprotection

HFIP cleavage from solid support: This procedure cleaves the peptide from 2-chlorotrityl resin without removing the sidechain protecting groups. The resin was transferred to a 5 mL fritted polypropylene cartridge and then washed with 5 mL DCM while being swirled by hand for 30 s and then drained by vacuum. The DCM wash was repeated twice, after which the resin was air dried by pulling vacuum through the cartridge. The resin was transferred to a 15 mL centrifuge tube, and a 12 mL cleavage cocktail of 20% 1,1,1,3,3,3-hexafluoroisopropanol (HFIP) in DCM was added to the resin. The mixture was shaken for 90 min on an orbital shaker, filtered through the fritted polypropylene cartridge into a 100 mL round bottom flask, and the resin was washed with 20% HFIP in DCM (3 times 1 mL) followed by DCM washes (3 times 1 mL). The filtrate and washings were dried under vacuum to yield an oily residue.

Solution phase peptide cyclization: The deprotected peptide from the HFIP cleavage step was dissolved in DMF (200 mL), and the mixture was transferred into a 500 mL round bottom flask. 2.0 mL of 1.0 M Oxyma in DMF and 2.0 mL of 1.0 M DIC in DMF were added to the round bottom flask, and the mixture was stirred at room temperature for 8 h. Then, the mixture was dried on a rotary evaporator at 70 °C to yield an oily residue.

Side chain deprotection: A 10 mL cleavage cocktail of 95% TFA, 2.5% TIPS, and 2.5% water was added to the peptide residue after the cyclization procedure. The mixture was stirred for 3 h and then dried under vacuum to yield an oily residue. Note that crystals of triphenylmethane, derived from trityl protecting groups may also appear.

Ether Precipitation: Diethyl ether (~20 mL) was added to the residue after sidechain deprotection, and the mixture was sonicated to obtain a white precipitate, which was transferred to a centrifuge tube and separated from the liquid phase by centrifugation for 3.0 min at 3.0 RCF resulting in a white pellet at the bottom of the centrifuge tube. The liquid phase was then decanted and the pellet was washed twice more with ~20 mL of diethyl ether, each time breaking up the pellet by sonication, and the crude product was allowed to air dry.

Reverse phase high performance liquid chromatography (RP-HPLC)

Preparative RP-HPLC was performed on a Waters Prep 2545 HPLC, equipped with a C18 (X-Bridge Peptide BEH 5µm, 19x 100 mm) column at a 17 mL/min flow rate monitored at a 214 nm wavelength. Crude samples were dissolved in water and filtered through a 0.2 µm filter before RP-HPLC purification. RP-HPLC was performed with water as the weak solvent and acetonitrile as the strong solvent. HPLC solvents were acidified with 0.1% trifluoracetic acid (see Table S5 for details). Fractions were analyzed for the product using UPLC-MS. Fractions containing the product were dried by lyophilization.

Table S5. HPLC gradients used for purification of synthesized compounds and final yields (accounting for trifluoroacetate anions ion paired with basic residues).

Compound	HPLC Gradient	Final Yield (%)
MC4H	10-50%	93 mg (42%)
MC4H-MeH	10-50%	87 mg (40%)
MC4H-MeA	10-50%	119 mg (53%)
MC4H-MeAMeH	10-50%	115 mg (51%)

*HPLC gradients used for purification of synthesized compounds and final yields (accounting for six ion-paired trifluoroacetate anions).

LC-MS data for reported peptides

Ultra-performance liquid chromatography (UPLC-MS)

Mass spectroscopy was performed using a Waters Acquity H-Class PLUS system equipped with a C18 (Acquity UPLC BEHEH 1.7 μm) column and TUV detector. Low-resolution electrospray ionization data were collected with an inline Waters SQD2 single quadrupole detector.

High Resolution electrospray-ionization mass spectrometry

High-resolution data were acquired on the Waters Synapt G2-Si ESI/LC-MS.

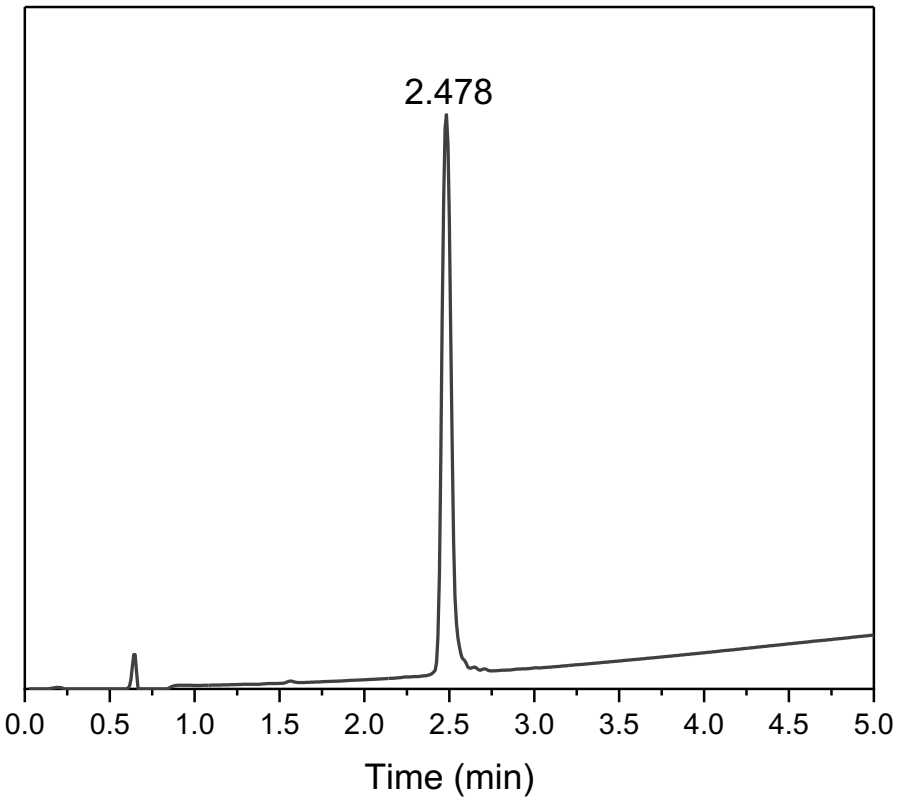

Figure S1. LC trace of **MC4H**. Gradient: 5-50% (MeCN/H_2O with 0.1% TFA) over 5 min.

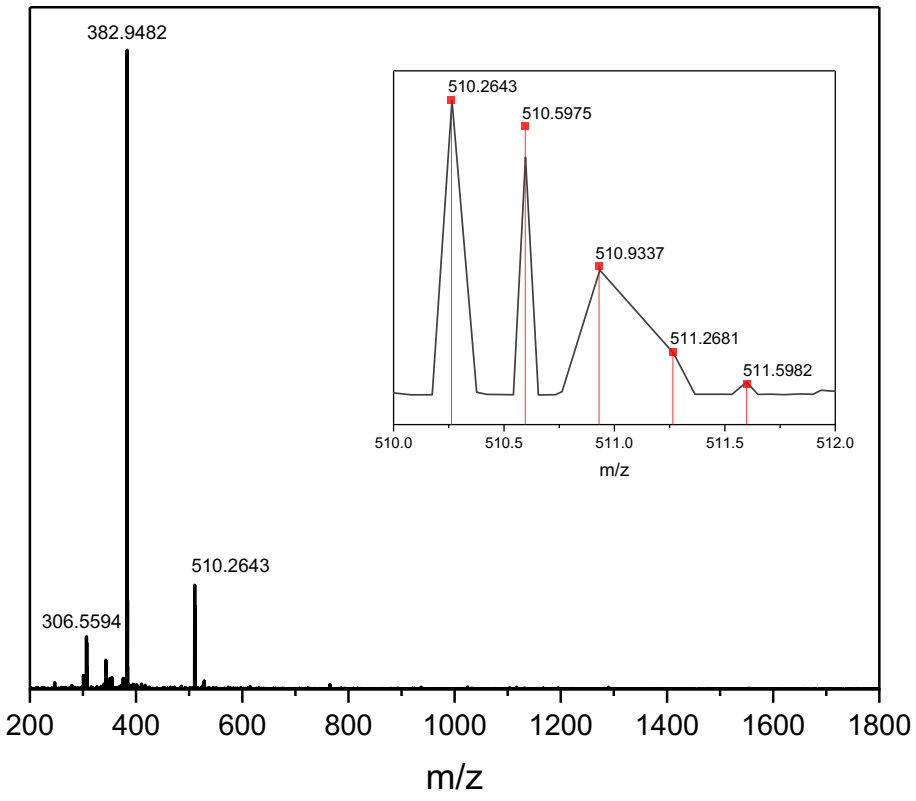

Figure S2. The mass spectrum (black) of **MC4H** with observed masses $[M+3H]^{3+}$ = 510.2643, $[M+4H]^{4+}$ = 382.9482, and $[M+5H]^{5+}$ = 306.5594. Experimental and simulated (red) spectrum for the $[M+3H]^{3+}$ ion are shown in the inset.

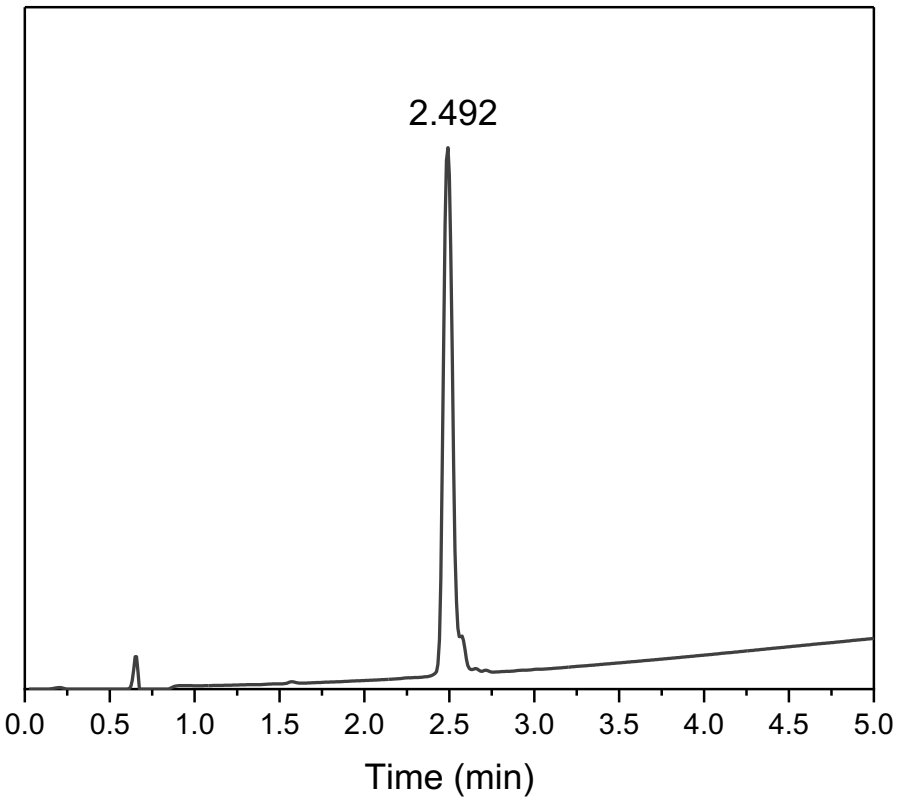

Figure S3. LC trace of **MC4H-MeH.** Gradient: 5-50% (MeCN/H_2O with 0.1% TFA) over 5 min.

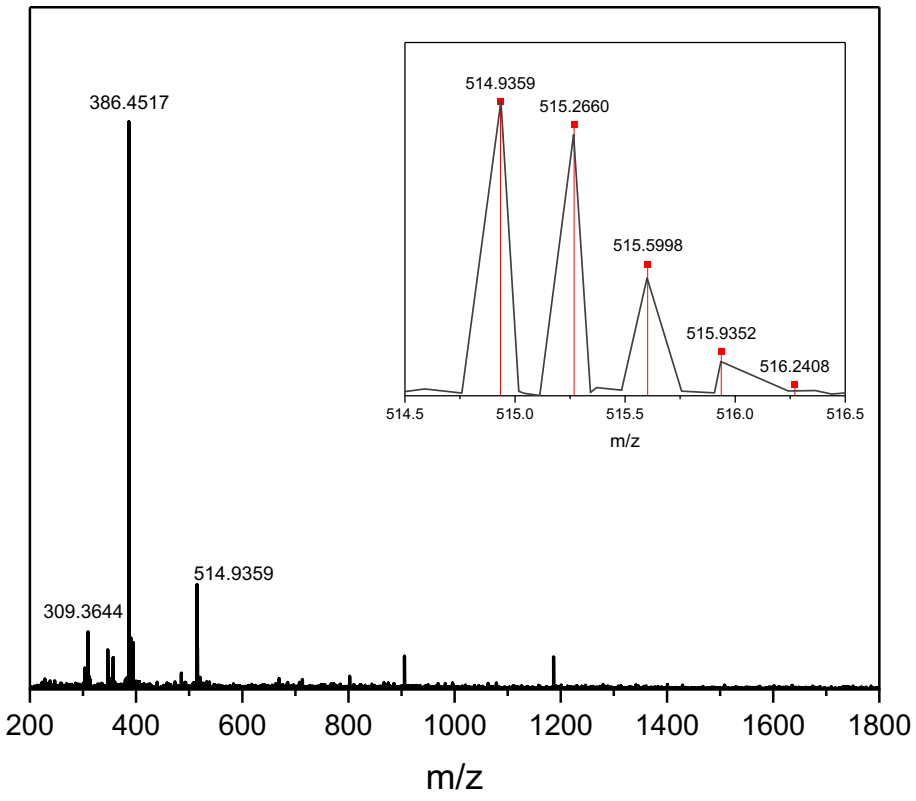

Figure S4. The mass spectrum (black) of **MC4H-MeH** with observed masses $[M+3H]^{3+}$ = 514.9359, $[M+4H]^{4+}$ = 386.4517, and $[M+5H]^{5+}$ = 309.3644. Experimental and simulated (red) spectrum for the $[M+3H]^{3+}$ ion are shown in the inset.

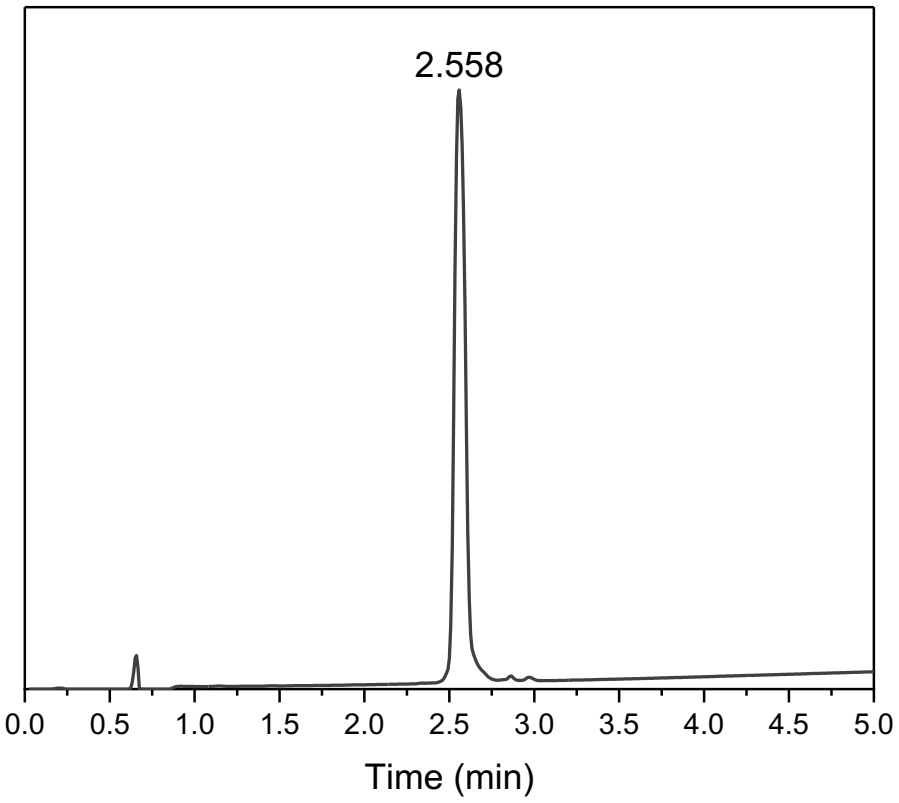

Figure S5. LC trace of **MC4H-MeA.** Gradient: 5-50% (MeCN/H_2O with 0.1% TFA) over 5 min.

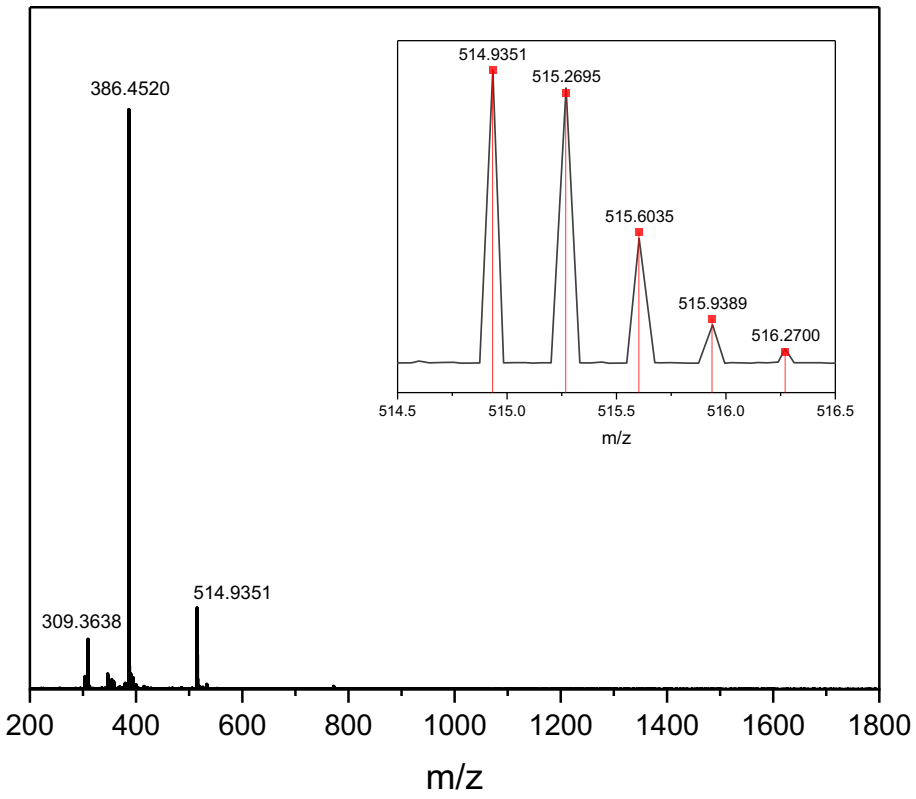

Figure S6. The mass spectrum (black) of **MC4H-MeA** with observed masses $[M+3H]^{3+}$ = 514.9351, $[M+4H]^{4+}$ = 386.4520, and $[M+5H]^{5+}$ = 309.3638. Experimental and simulated (red) spectrum for the $[M+3H]^{3+}$ ion are shown in the inset.

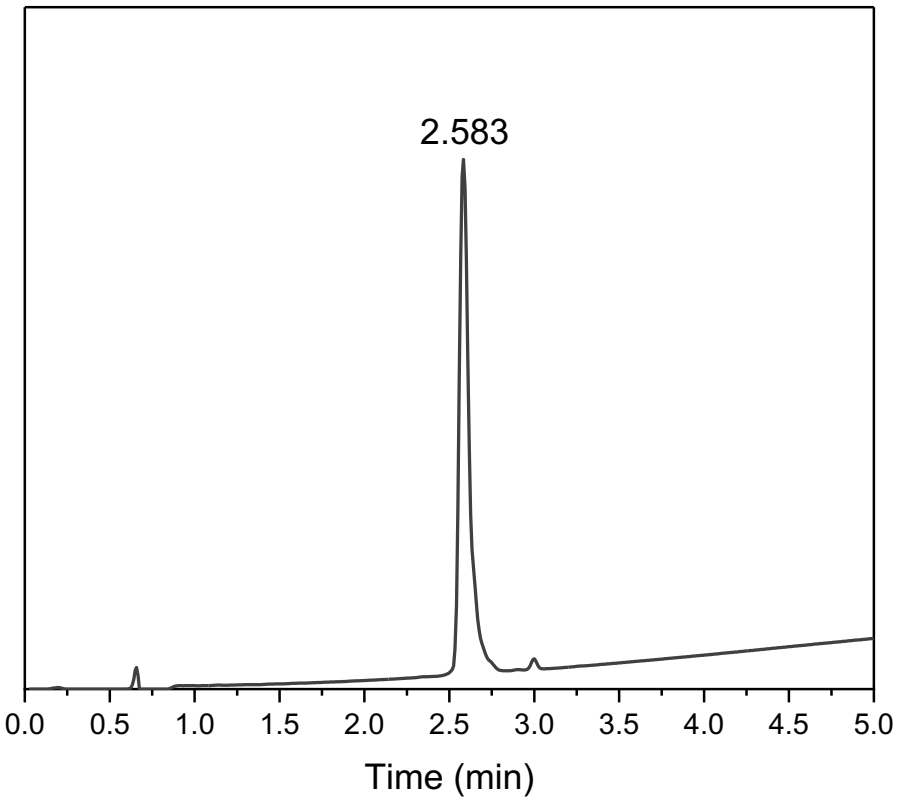

Figure S7. LC trace of **MC4H-MeAMeH.** Gradient: 5-50% (MeCN/H_2O with 0.1% TFA) over 5 min.

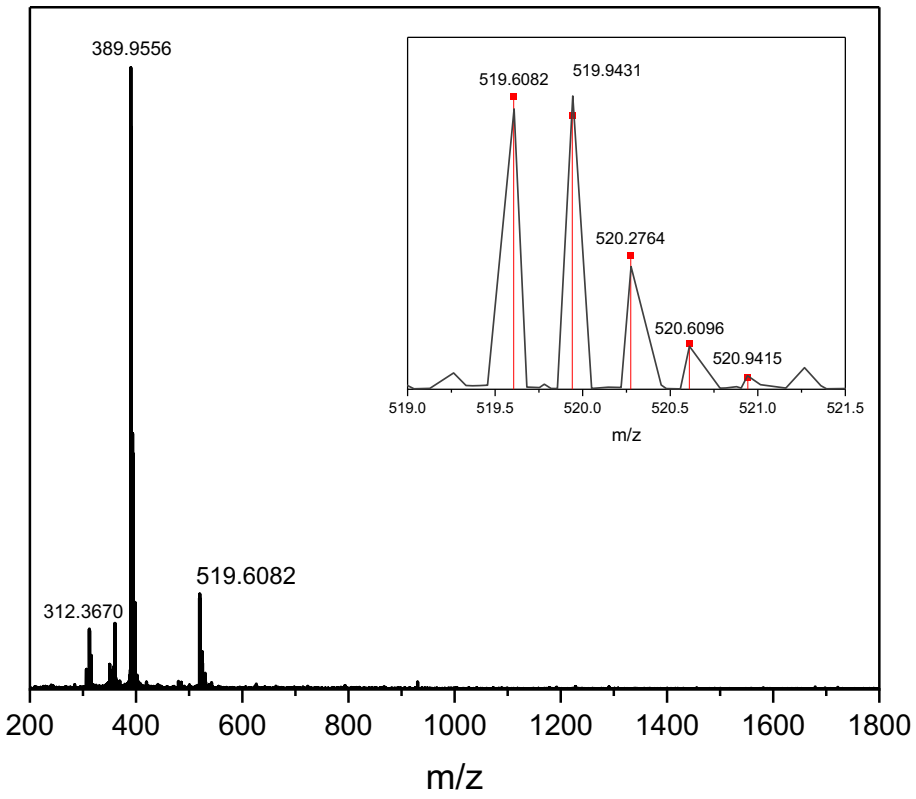

Figure S8. The mass spectrum (black) of **MC4H-MeAMeH** with observed masses $[M+3H]^{3+}$ = 519.6082, $[M+4H]^{4+}$ = 389.9556, and $[M+5H]^{5+}$ = 312.3670. Experimental and simulated (red) spectrum for the $[M+3H]^{3+}$ ion are shown in the inset.

Nuclear magnetic resonance (NMR) spectroscopy

^{1}H 1D NMR spectra were measured on a Bruker Avance III 500 MHz console using Topspin3.7.0. Peptide samples were dissolved in 90% H_2O and 10% D_2O. The temperature was held at 280 K with a variable temperature module and the peaks are referenced to TMS. 1D ^{1}H water suppressed spectra were acquired using the Bruker parameter file ZGESGP having excitation sculpting for the water peak selection and suppression.[1] Typical spectra were acquired with a sweep width of 12ppm, 32 scans, 3 second recycle delays and 1.5s of data acquisition. All spectra below were processed and analyzed with either Topspin3.7.0 or Mnova software.

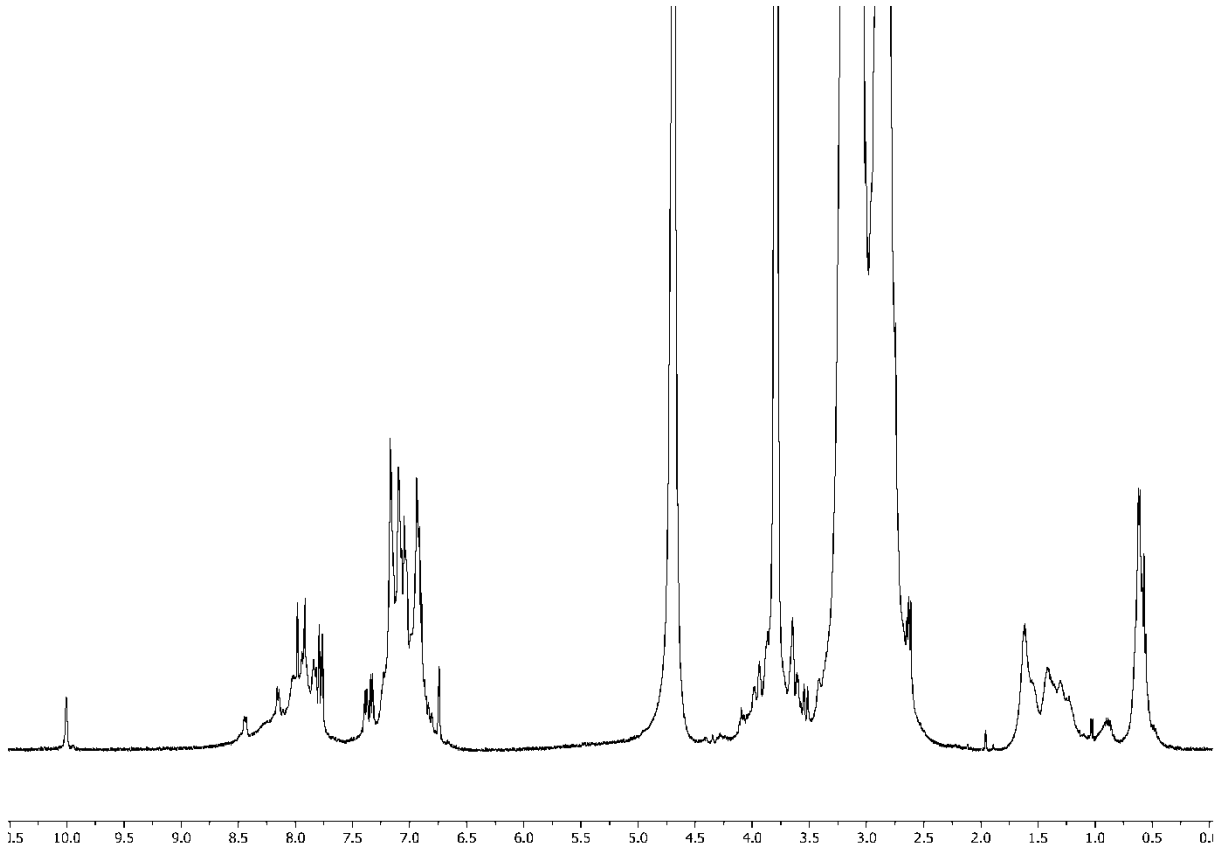

Figure S9. ^{1}H NMR spectrum of **MC4H**. Sample dissolved in 0.1 M HEPES pH 7.0 with 10% D_2O and 90% H_2O at 280 K.

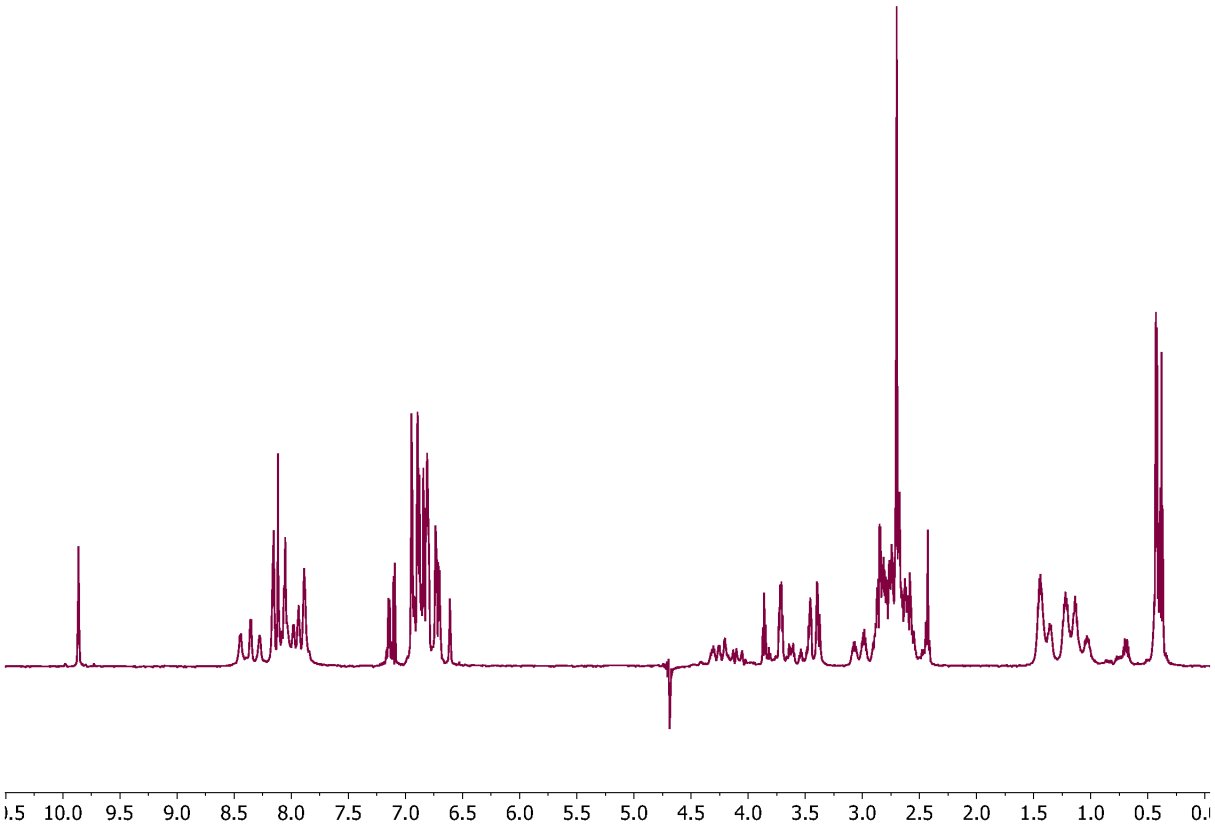

Figure S10. ^{1}H NMR spectrum of **MC4H**. Sample dissolved in 0.05 M potassium phosphate pH 6.90 with 10% D_2O and 90% H_2O at 280 K.

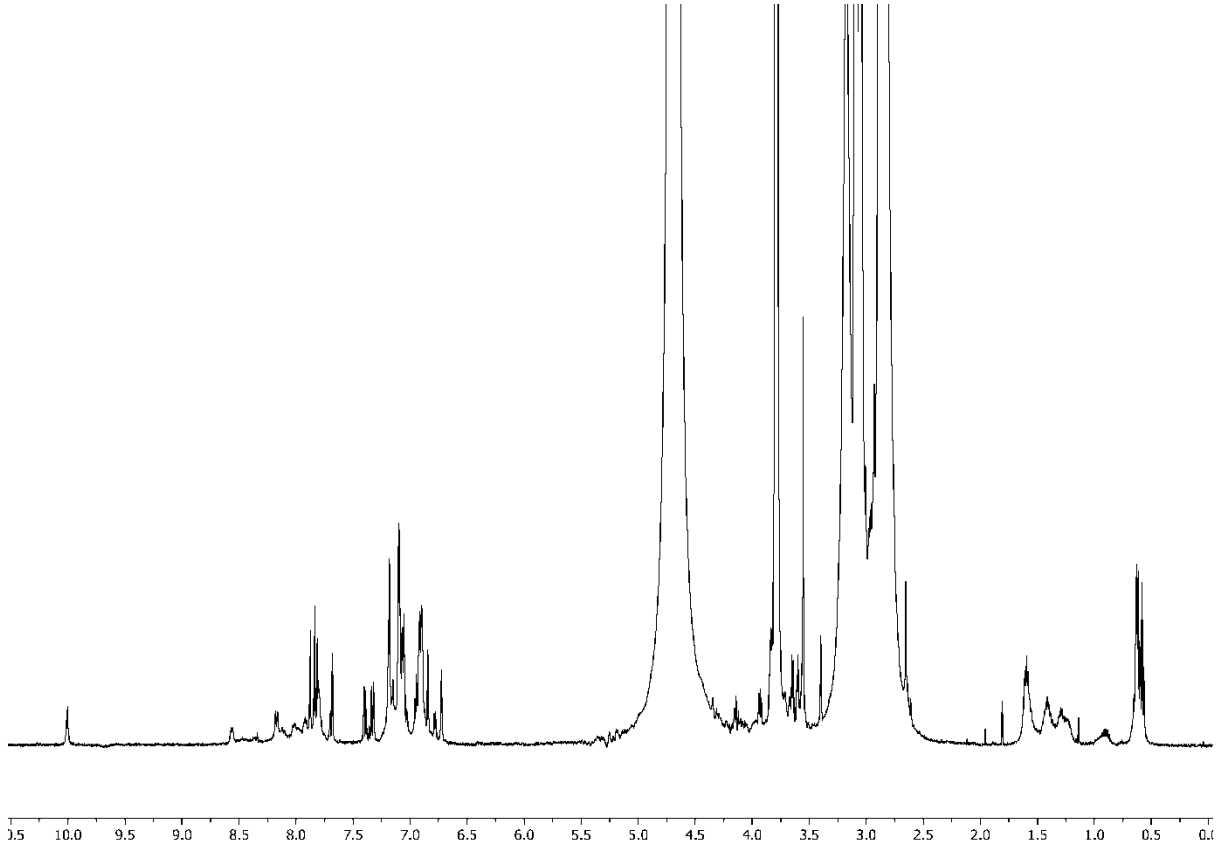

Figure S11. ^{1}H NMR spectrum of **MC4H-MeH**. Sample dissolved in 0.1 M HEPES pH 7.0 with 10% D_2O and 90% H_2O at 280 K.

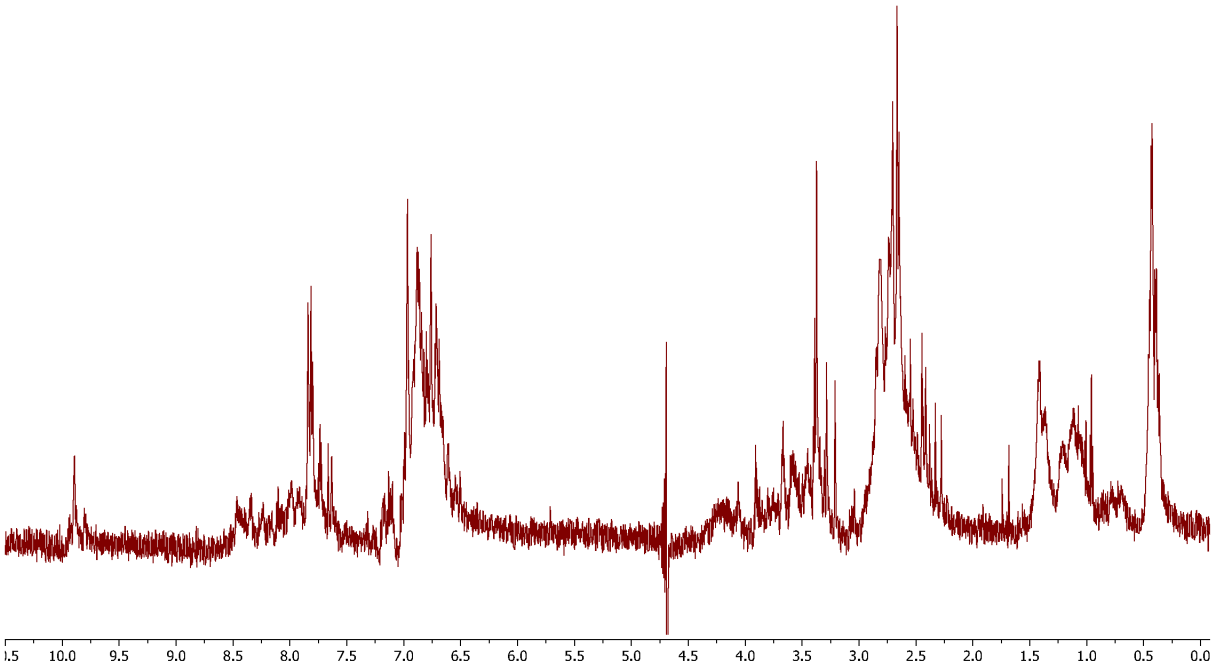

Figure S12. ^{1}H NMR spectrum of **MC4H-MeH**. Sample dissolved in 0.05 M potassium phosphate pH 6.90 with 10% D_2O and 90% H_2O at 280 K. This peptide has poor solubility, resulting in a noisy spectrum.

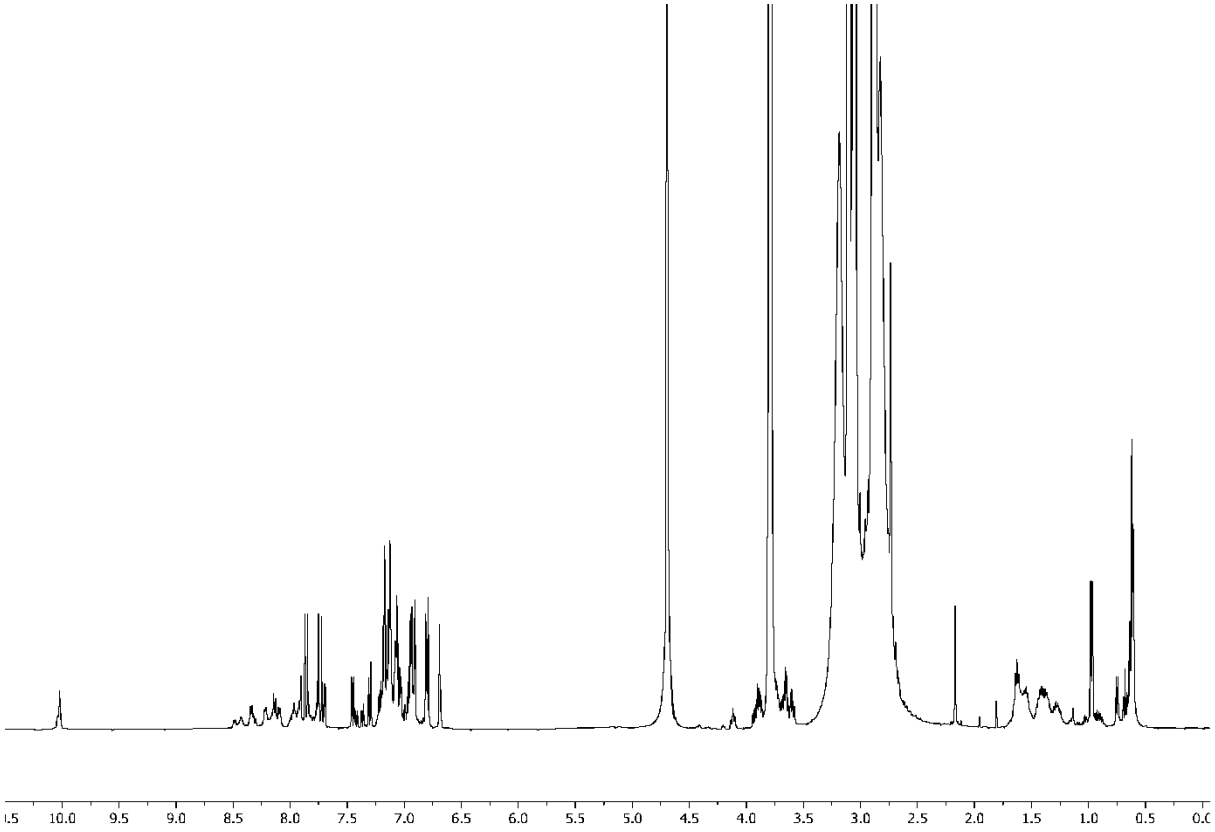

Figure S13. ^{1}H NMR spectrum of **MC4H-MeA**. Sample dissolved in 0.1 M HEPES pH 7.0 with 10% D_2O and 90% H_2O at 280 K.

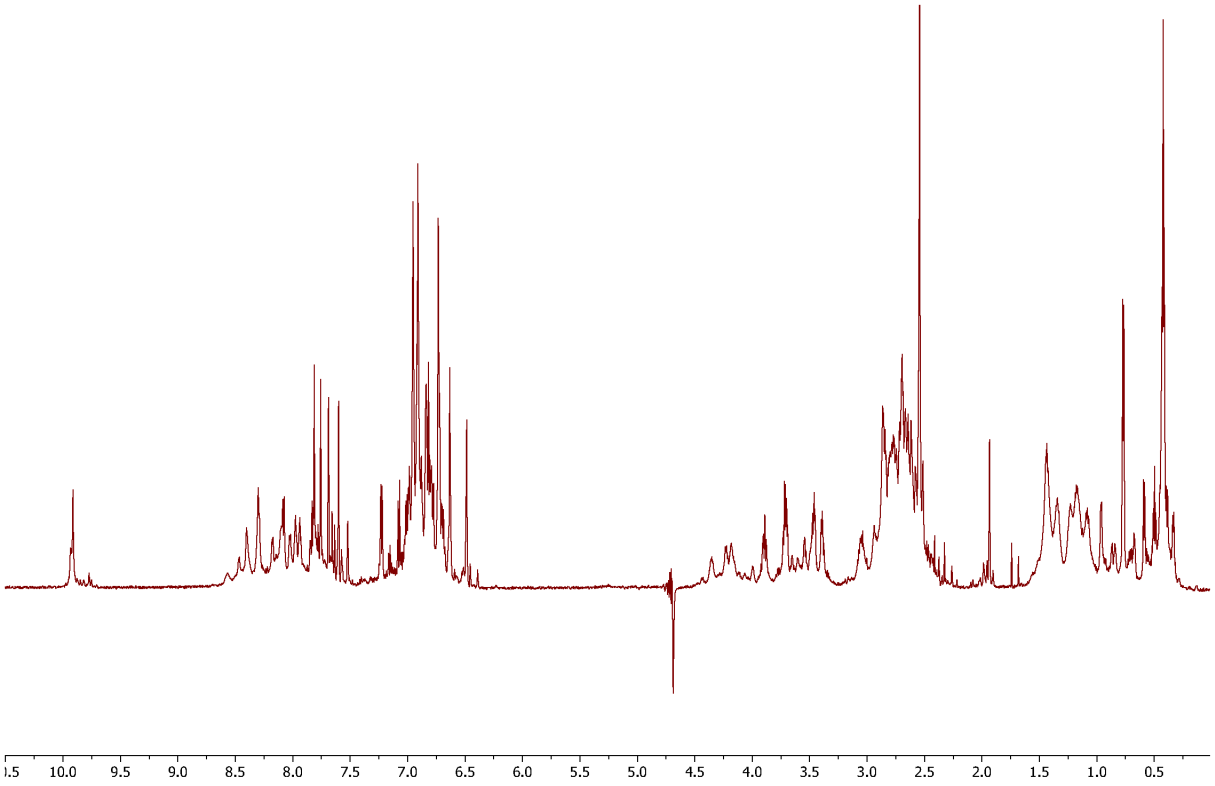

Figure S14. ^{1}H NMR spectrum of **MC4H-MeA**. Sample dissolved in 0.05 M potassium phosphate pH 6.90 with 10% D_2O and 90% H_2O at 280 K.

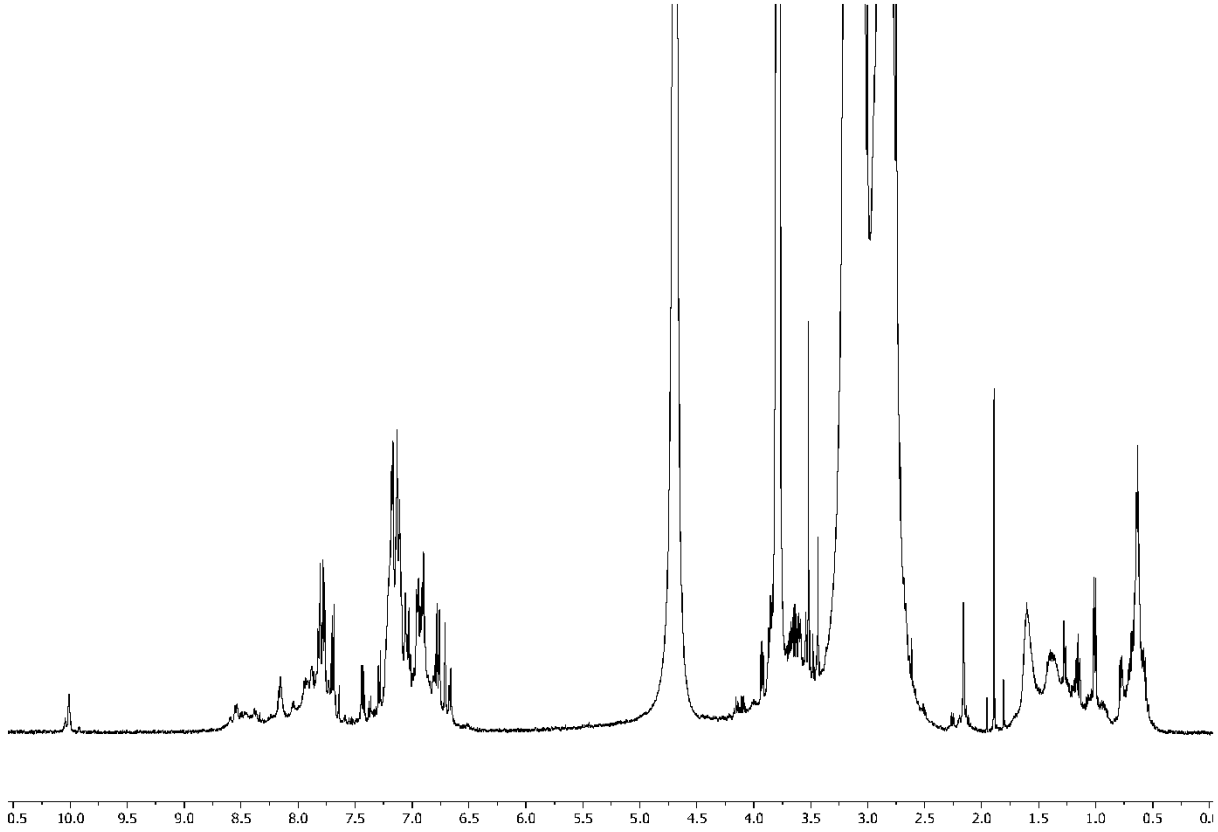

Figure S15. ^{1}H NMR spectrum of **MC4H-MeAMeH**. Sample dissolved in 0.1 M HEPES pH 7.0 with 10% D_2O and 90% H_2O at 280 K.

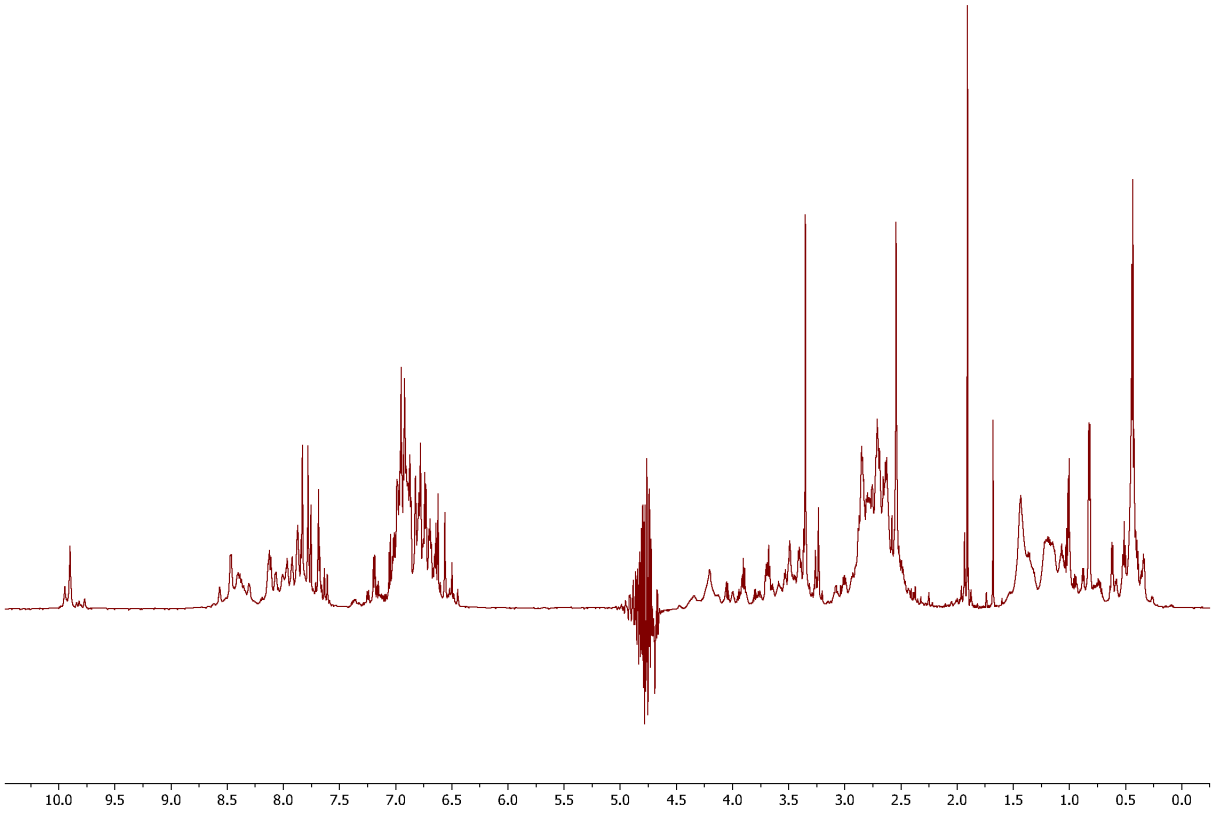

Figure S16. ^{1}H NMR spectrum of **MC4H-MeAMeH**. Sample dissolved in 0.05 M potassium phosphate pH 6.90 with 10% D_2O and 90% H_2O at 280 K.

Diffusion NMR methods and processing

The diffusion NMR spectra were acquired using a stimulated echo with bipolar gradients and 3-9-19 water suppression element according to the Bruker pulse program (stebpgp1s19). Each 1D was recorded by linearly incrementing the PFG from 5-95% over 32 steps where the maximum applied gradient strength is 54.5 G/cm. The typical allowed diffusion time (big delta) Δ = d20 = 120 ms, δ (little delta) for Eddy currents = 2 ms, 12 ppm sweep width, 32 scans per increment and 3 second recycle delay.[2] Each individual 1D NMR spectrum, as a function of applied PFG strength, was processed and integrated in MNova. The integrated regions were fitted within *OriginPro* according to eq S2.

The diffusion data were fitted to the classic Stejskal and Tanner analytical equation for a stimulated-echo bipolar pulsed field gradient experiment (eq S2).[43]

$$I = I_0 \times e^{-D\gamma^2\delta^2 g^2\left(\Delta-\frac{\delta}{3}\right)} \qquad \text{(eq S2)}$$

where I = observed intensity
I_0 = reference intensity unattenuated
D = diffusion rate ($cm^2\ s^{-1}$)
g = applied Z-gradient strength ($G\ cm^{-1}$)
γ = gyromagnetic ratio of the observed nucleus
δ = gradient pulse duration (0.002 s)
Δ = Stejskal-Tanner diffusion delay (0.120 s)

The diffusion coefficient, D is roughly proportional to $M^{-\alpha}$, with α being a function of the molecular shape.[3] α is 1/3 for a perfect sphere and 1 for an infinite rod. Experimentally, it is shown that folded polypeptides have α ~ 0.39, close to the ideal value of 1/3, whereas unfolded chains have α ~ 0.58. Thus, $0.33 < \alpha < 0.58$ is reasonable for peptides. While **MC4H** has a higher aspect ratio than a perfect sphere, it is closer to a globular fold than a linear rod, and so we apply α = 1/3. Since spectroscopic data show all peptides in this work are folded, we assume that the mass ratios of peptides follow the relationship shown by eq S3. We can adjust eq. S3 to account for the mass differences between the reference and the sample to yield eq. S4.

$$\frac{D_1}{D_2} = \left(\frac{M_2}{M_1}\right)^{1/3} \qquad \text{(eq S3)}$$

where D_1 = diffusion rate of species 1 ($m^2\ s^{-1}$)
D_2 = diffusion rate of species 2 ($m^2\ s^{-1}$)
M_1 = molecular mass of species 1 ($g\ mol^{-1}$)
M_2 = molecular mass of species 2 ($g\ mol^{-1}$)

$$\langle O \rangle = \frac{\left(\frac{D_{ref}}{D_s}\right)^3 \times M_{ref}}{M_{mono}} \qquad \text{(eq S4)}$$

where D_{ref} = diffusion rate of the monomeric reference species ($m^2\ s^{-1}$)
D_s = diffusion rate of the sample species ($m^2\ s^{-1}$)
M_{ref} = molecular mass for a monomer of the reference species ($g\ mol^{-1}$)
M_{mono} = expected mass for a monomer of the sample species ($g\ mol^{-1}$)
$\langle O \rangle$ = average oligomeric state

Table S6. Oligomerization states of peptides determined by diffusion NMR spectroscopy

Sample	D ($m^2/s \cdot 10^{-10}$)	$\langle O \rangle^a$	%dimer
trpzip2	2.8	1.00	0
MC4H	2.25	2.03	100%
MC4H-MeH	2.43	1.60	60%
MC4H-MeA	2.60	1.30	30%
MC4H-MeAMeH	2.59	1.31	31%

[a] $\langle O \rangle$ can be defined as the weighted average of dimer and monomer: $\frac{2[D]+[M]}{[D]+[M]}$ or alternatively $1 + f_D$ where f_D is the mole fraction of D, or $\frac{[D]}{[D]+[M]}$. For example, a solution composed of 50% dimers correspond to an observed oligomer state of 1.5.

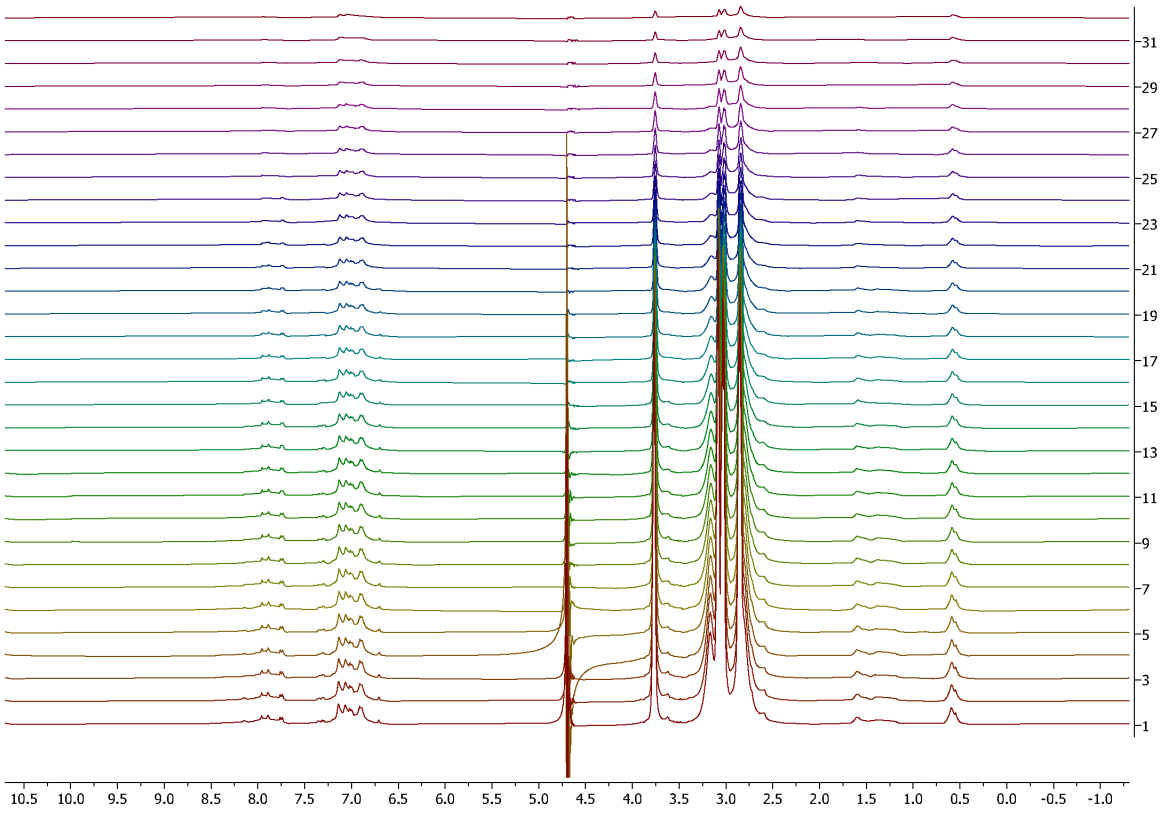

Figure S17. ^{1}H NMR spectra of **MC4H** at different applied gradient strengths. Sample dissolved in 0.1 M HEPES pH 7.0 in 10% D_2O and 90% H_2O at 280 K.

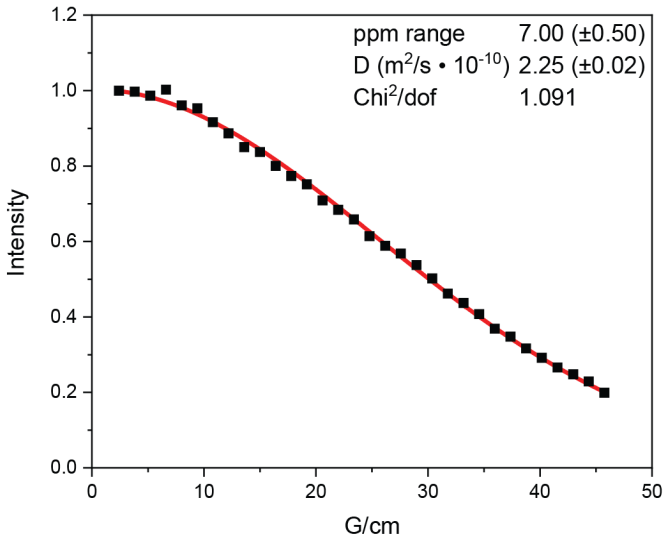

Figure S18. Fitting the integrated peaks for **MC4H** from 6.50-7.50 ppm as a function of applied Z-gradient strength, using equation S2.

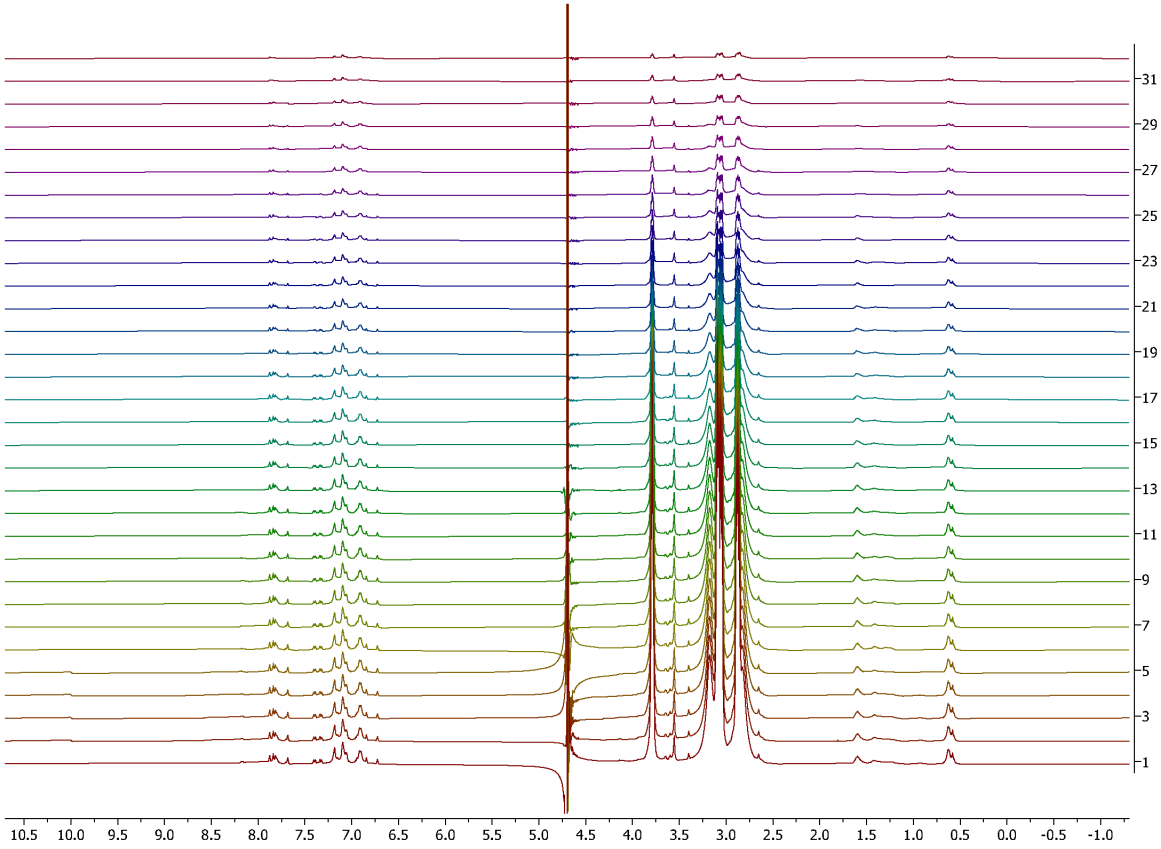

Figure S19. ^{1}H NMR spectra of **MC4H-MeH** at different applied gradient strengths. Sample dissolved in 0.1 M HEPES pH 7.0 in 10% D_2O and 90% H_2O at 280 K.

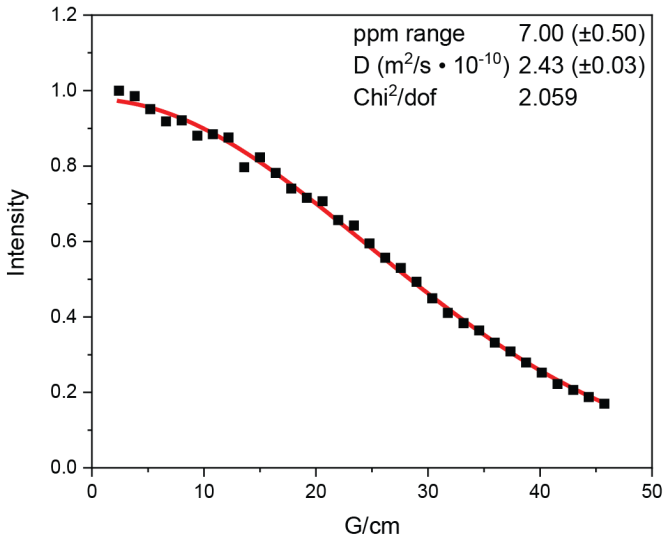

Figure S20. Fitting the integrated peaks for **MC4H-MeH** from 6.50-7.50 ppm as a function of applied Z-gradient strength, using equation S2.

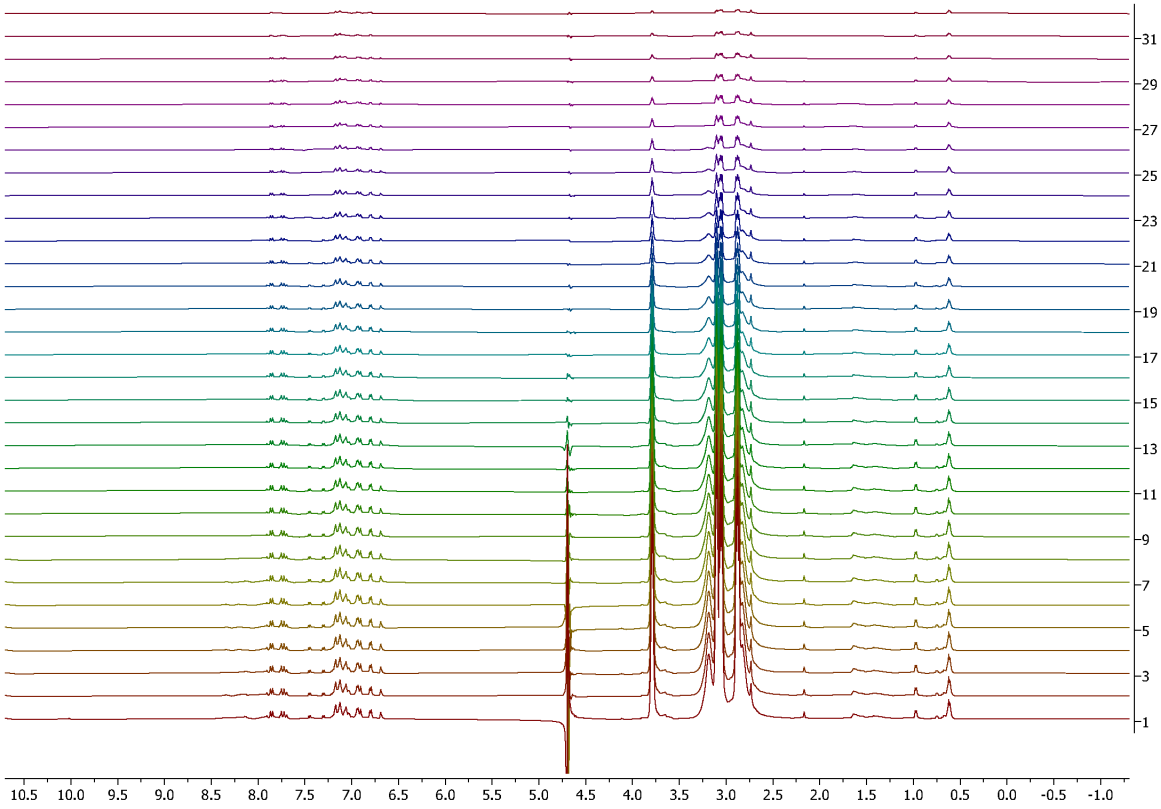

Figure S21. ^{1}H NMR spectra of **MC4H-MeA** at different applied gradient strengths. Sample dissolved in 0.1 M HEPES pH 7.0 in 10% D_2O and 90% H_2O at 280 K.

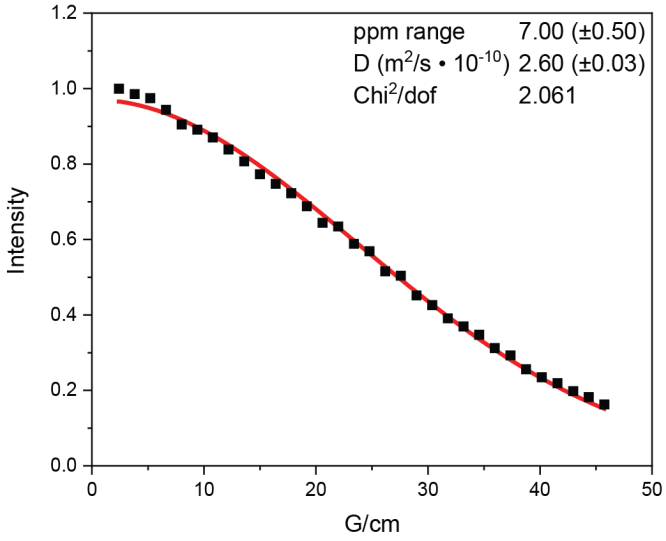

Figure S22. Fitting the integrated peaks for **MC4H-MeA** from 6.50-7.50 ppm as a function of applied Z-gradient strength, using equation S2..

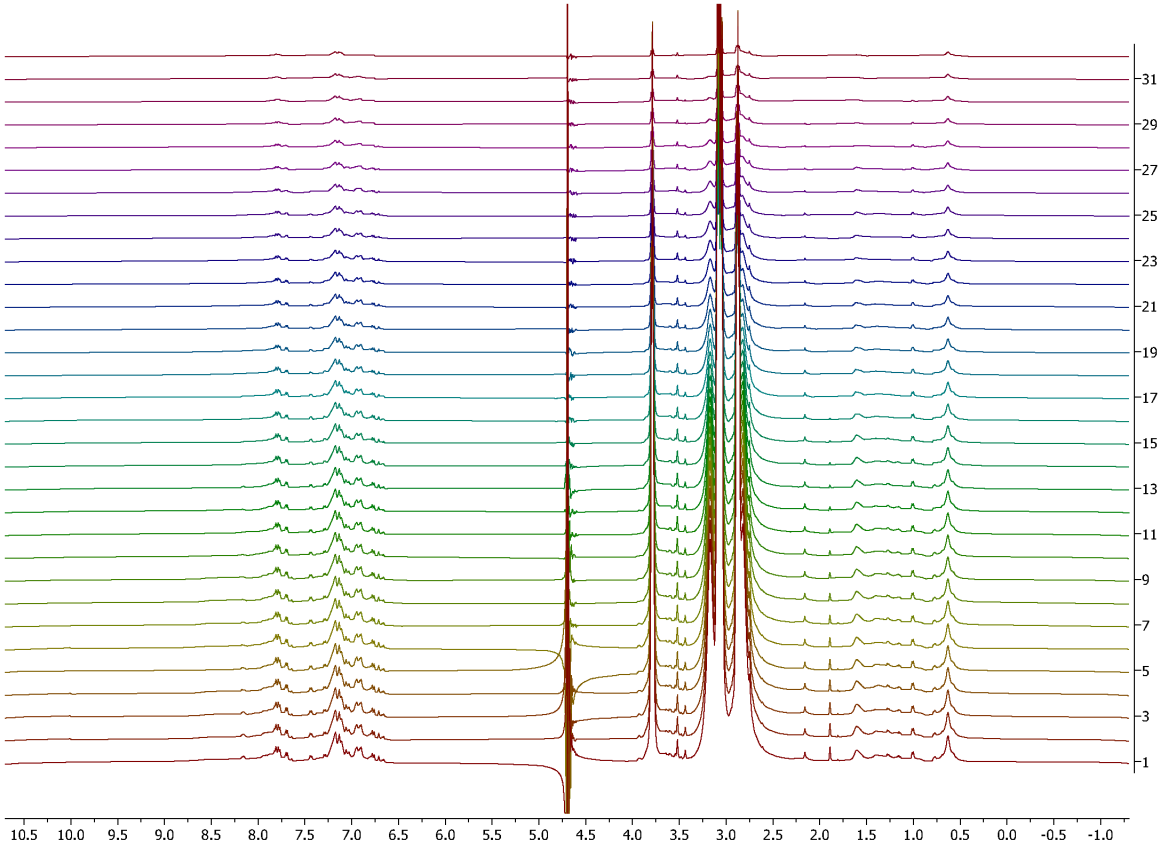

Figure S23. ^{1}H NMR spectra of **MC4H-MeAMeH** at different applied gradient strengths. Sample dissolved in 0.1 M HEPES pH 7.0 in 10% D_2O and 90% H_2O at 280 K.

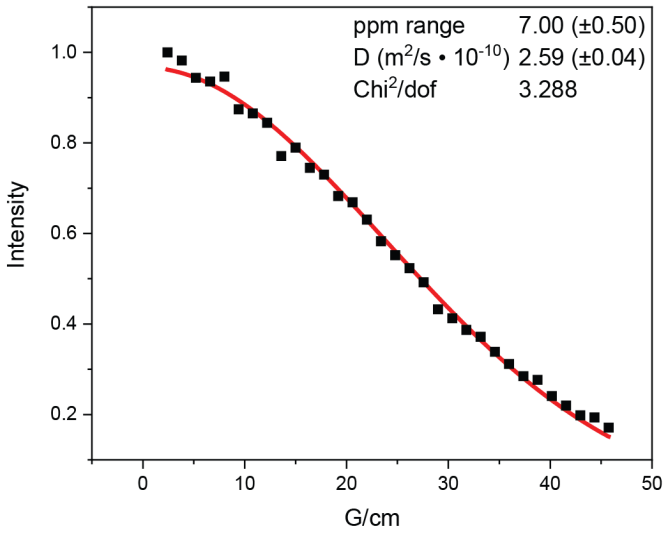

Figure S24. Fitting the integrated peaks for **MC4H-MeAMeH** from 6.50-7.50 ppm as a function of applied Z-gradient strength, using equation S2.

Circular dichroism spectroscopy

The secondary structures of the peptide samples were evaluated using circular dichroism spectroscopy on a Jasco J-1500 Circular Dichroism Spectrophotometer. Samples of 400 μL volume and 0.1 mg/mL concentration in 10 mM HEPES pH. 7.0 were prepared and transferred to a 1.0 mm pathlength quartz cuvette. The ellipticity of each sample was measured from 210–350 nm wavelength, with 5 acquisitions at 25° C and at a scanning speed of 100 nm/min. The ellipticity (θ / mdeg) was converted to mean molar ellipticity (Φ / mdeg M^{-1} cm^{-1}) using the equation reported by Kelly et al (eq S6). [5]

$$\Phi = \frac{\theta \cdot M}{10 \cdot n \cdot l \cdot C} \qquad \text{(eq S6)}$$

θ is the ellipticity in mdeg, M is the molecular mass of the sample, n is the number of amide bonds in the structural formula, l is the optical path length in cm, and C is the concentration in mg/mL.

Variable temperature CD data were fit to a model for a two-state transition between a folded dimer (D) and unfolded monomer (M).[6]

$$2M \leftrightharpoons D \qquad \text{(eq S7)}$$

$$K(T) = \frac{[D]_{eq}}{[M]_{eq}^{\,2}} \qquad \text{(eq S8)}$$

At the melting temperature, T_m, there are equal amounts of folded and unfolded species, and since D carries two copies of folded chains:

$$[M]_{T_m} = 2[D]_{T_m} \qquad \text{(eq S9)}$$

From mass balance, where c is the total concentration of peptide monomers, we obtain:

$$c = [M] + 2[D] \qquad \text{(eq S10)}$$

$$c = 2[M]_{T_m} \qquad \text{(eq S11)}$$

Substitution of equations S9 and S11 into S8, the equilibrium constant at T_m is:

$$K(T_m) = \frac{1}{c} \qquad \text{(eq S12)}$$

$$\Delta G(T_m) = RT_m \ln c \qquad \text{(eq S13)}$$

Substitution of eq S13 into the Gibbs-Helmholtz equation yields $K(T)$ as a function of T_m:

$$\frac{\Delta G(T)}{T} - \frac{\Delta G(T_m)}{T_m} = \Delta H \left(\frac{1}{T} - \frac{1}{T_m}\right) \qquad \text{(eq S14)}$$

$$-\Delta G(T) = \Delta H \left(\frac{T}{T_m} - 1\right) - RT \ln c \qquad \text{(eq S15)}$$

$$K(T) = \exp\left\{\frac{\Delta H}{RT}\left(\frac{T}{T_m} - 1\right) - \ln c\right\} \qquad \text{(eq S16)}$$

Next, $K(T)$ needs to be related to the observed molar ellipticity $\Phi(T)$, which directly reports on $[D]_{eq}$. From equation S8 and S10, $[D]_{eq}$ at any temperature for a given c is calculated by:

$$K = \frac{[D]_{eq}}{(c-2[D]_{eq})^2} \qquad \text{(eq S17)}$$

$$[D]_{eq} = \frac{(4cK+1)-\sqrt{8cK+1}}{8K} \qquad \text{(eq S18)}$$

As the model assumes only D is folded, the fraction of folded species, α, is:

$$\alpha = \frac{2[D]_{eq}}{c} = \frac{(4cK+1)-\sqrt{8cK+1}}{4cK} \qquad \text{(eq S19)}$$

For convenience, the individual terms of equation S19 are grouped below as:

$$q = 4cK + 1 \qquad \text{(eq S20)}$$
$$e = \sqrt{8cK + 1} \qquad \text{(eq S21)}$$
$$d = 4cK \qquad \text{(eq S22)}$$
$$\alpha = (q - e)/d \qquad \text{(eq S23)}$$

Finally, the observed molar ellipticity at each temperature, $\Phi(T)$, is related to α by:

$$\Phi(T) = \alpha\Phi_{folded} + (1 - \alpha)\Phi_{unfolded} \qquad \text{(eq S24)}$$

Using OriginPro, equations S16, S20-24 were fit to experimental $\Phi(T)$ to extract the parameters ΔH, T_m, Φ_{folded}, and $\Phi_{unfolded}$.

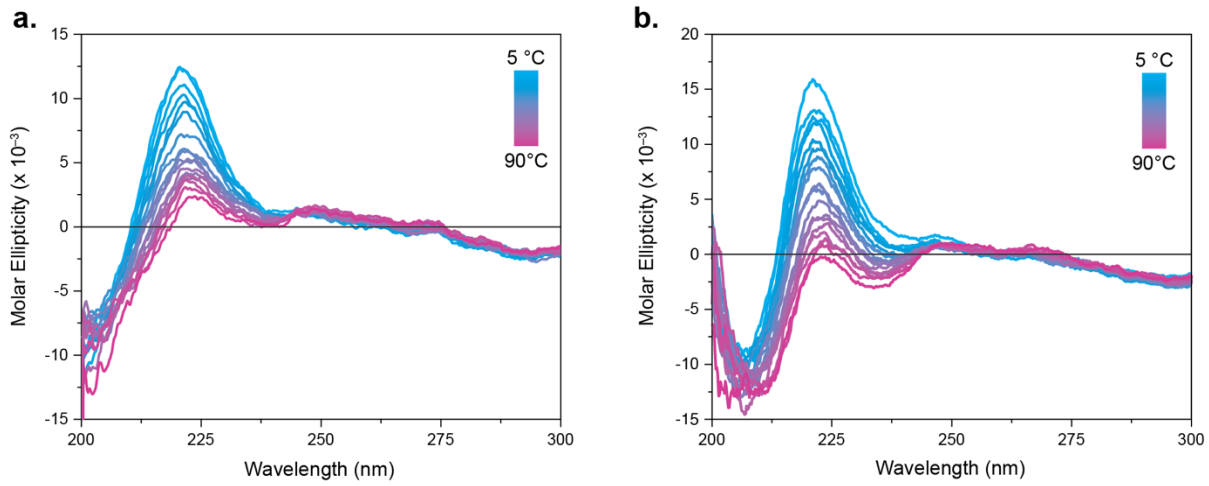

Figure S25. Variable temperature CD spectra of (a) **MC4H** and (b) **MC4H-MeH**.

2D NMR spectroscopy

Peptides were dissolved in 10% D_2O and 90% H_2O and buffered with 0.05 M potassium phosphate buffer pH 6.90. 1D ^1H NMR with excitation sculpting water suppression, 2D-NOESY and 2D-TOCSY spectra were obtained with a Bruker AVIII 750 MHz running Topspin 3.6.2 software. The temperature was calibrated to 280 K with neat methanol and gradient selection and excitation sculpting was used for water suppression. The 1D ^1H NMR was acquired using the Bruker parameter file ZGESGP. The 2D-NOESY were acquired (mixing time = 300 ms) with 16 ppm sweep widths, 16384x1024 complex points in t2xt1 and 16 scans per increment. The starting parameter file calls within Topspin would be NOESYESGPPH and TOCSYESGPPH. Recycle delays between scans were set to 3 s and the t1 acquisition mode was defined as STATES-TPPI. 2D-TOCSY were acquired under similar conditions with DIPSI2 (mixing = 70 ms) and a radio-frequency field of 8 kHz. All spectra were processed, viewed, and assigned in MestReNova. The NOESY peaks were manually selected and assigned in MestReNova. Manual NOE assignments/distances were utilized for structure determination starting from CYANA 3.9.8 and further refined in AMBER 14.

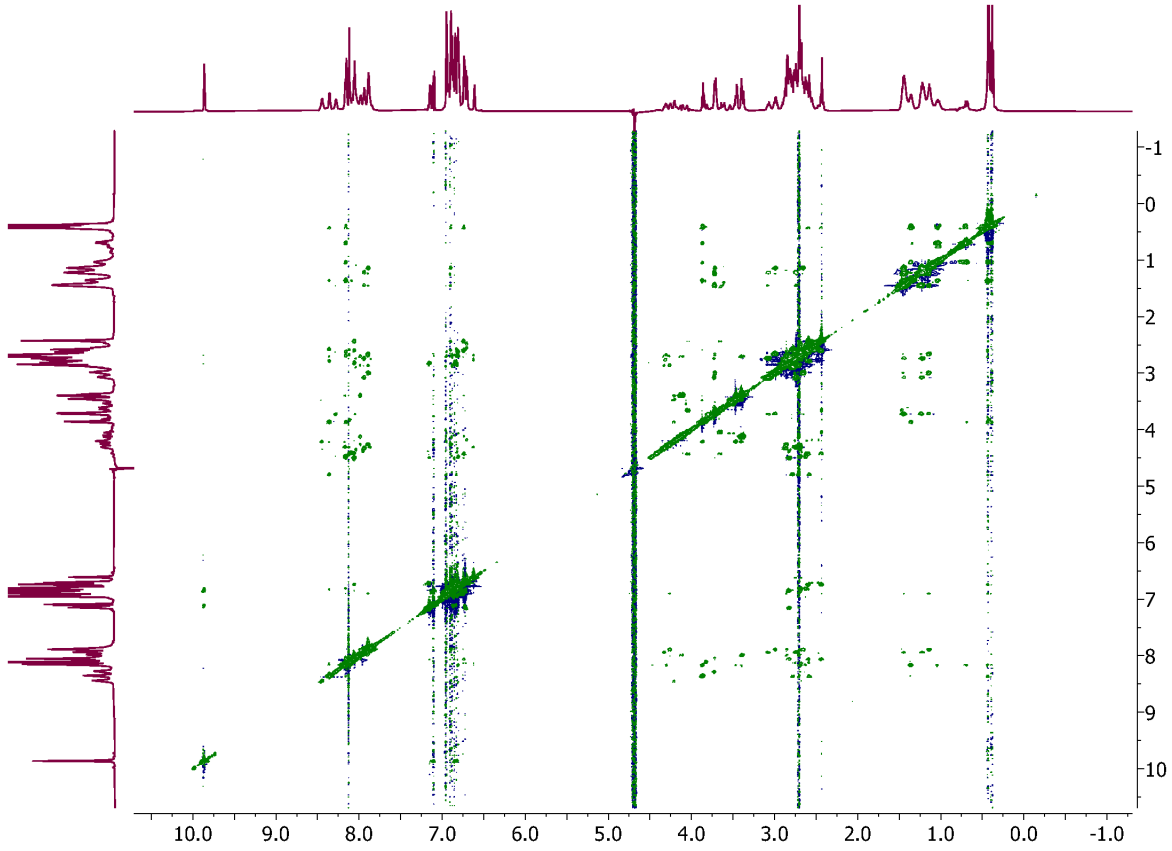

Figure S26. 2D NOESY for **MC4H**. Sample dissolved in 0.05 M potassium phosphate buffer pH 6.90 with 10% D_2O and 90% H_2O at 280 K.

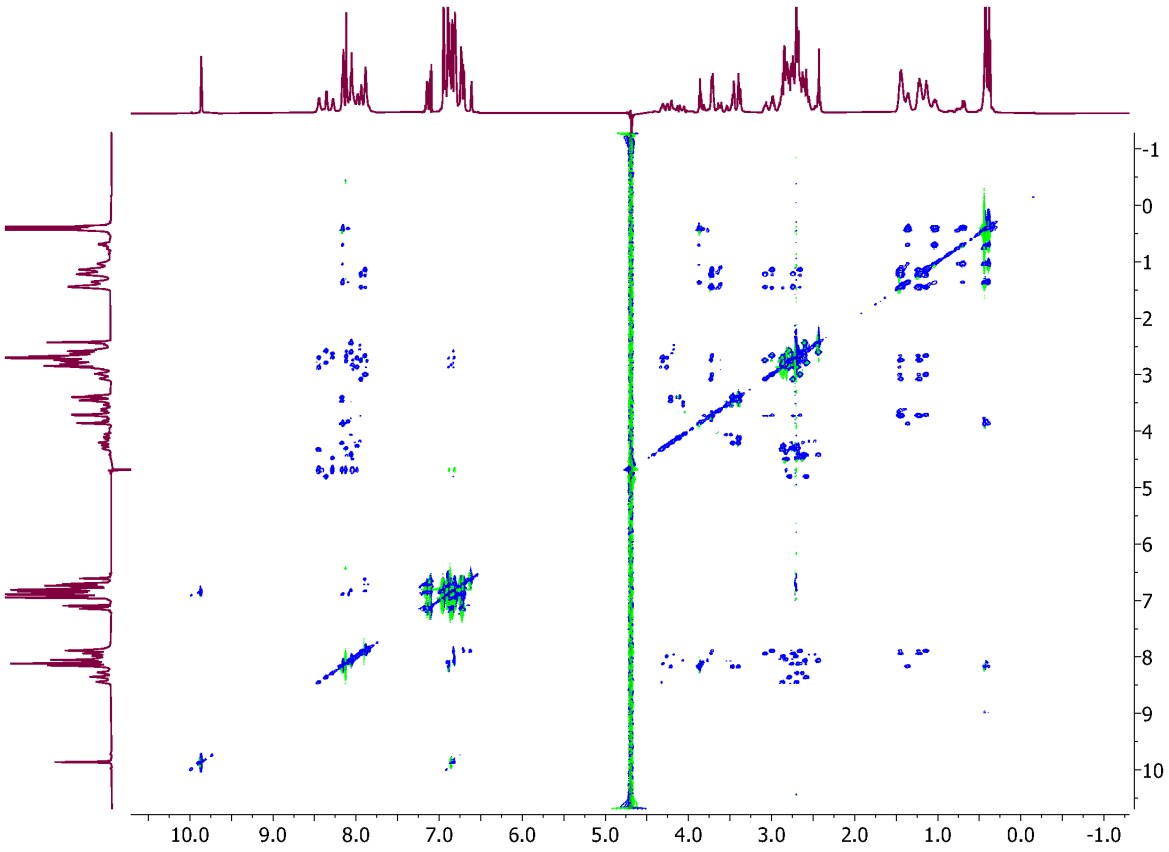

Figure S27. 2D TOCSY for **MC4H**. Sample dissolved in 0.05 M potassium phosphate buffer pH 6.90 with 10% D_2O and 90% H_2O at 280 K.

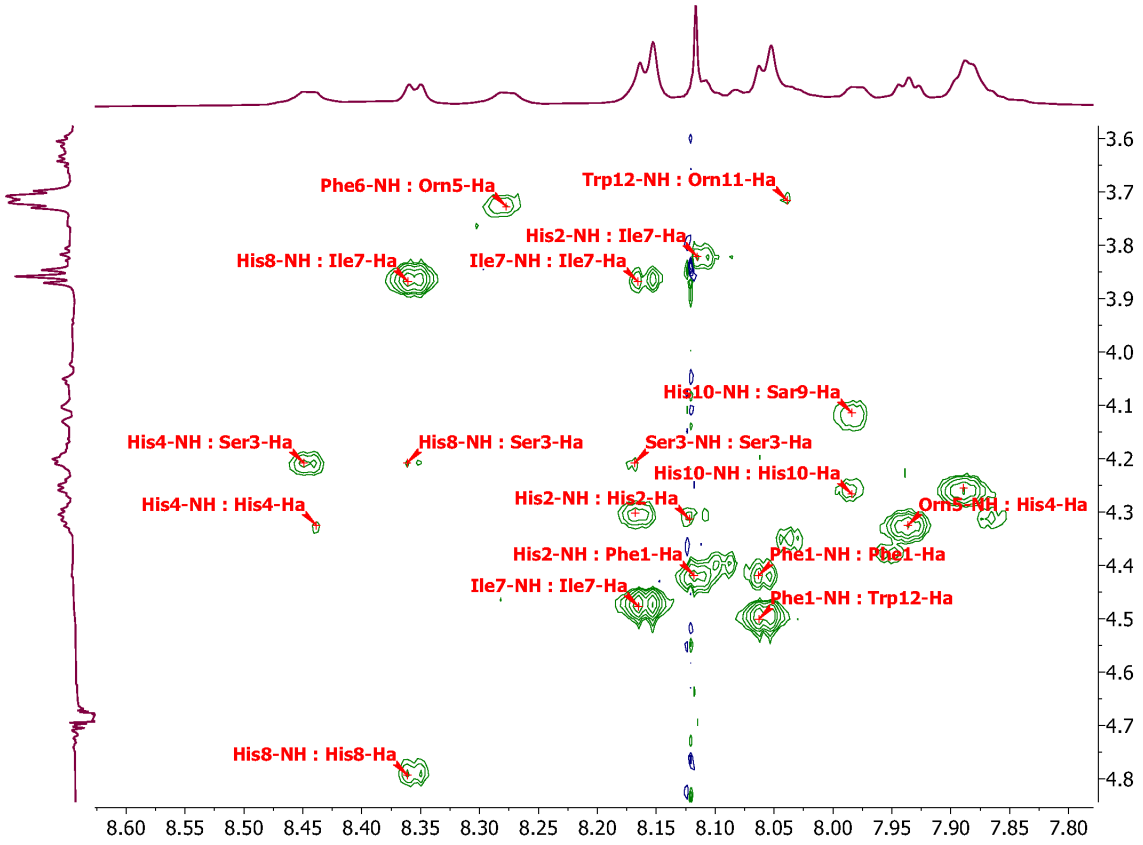

Figure S28. NOESY NH-Hα crosspeaks for **MC4H**.

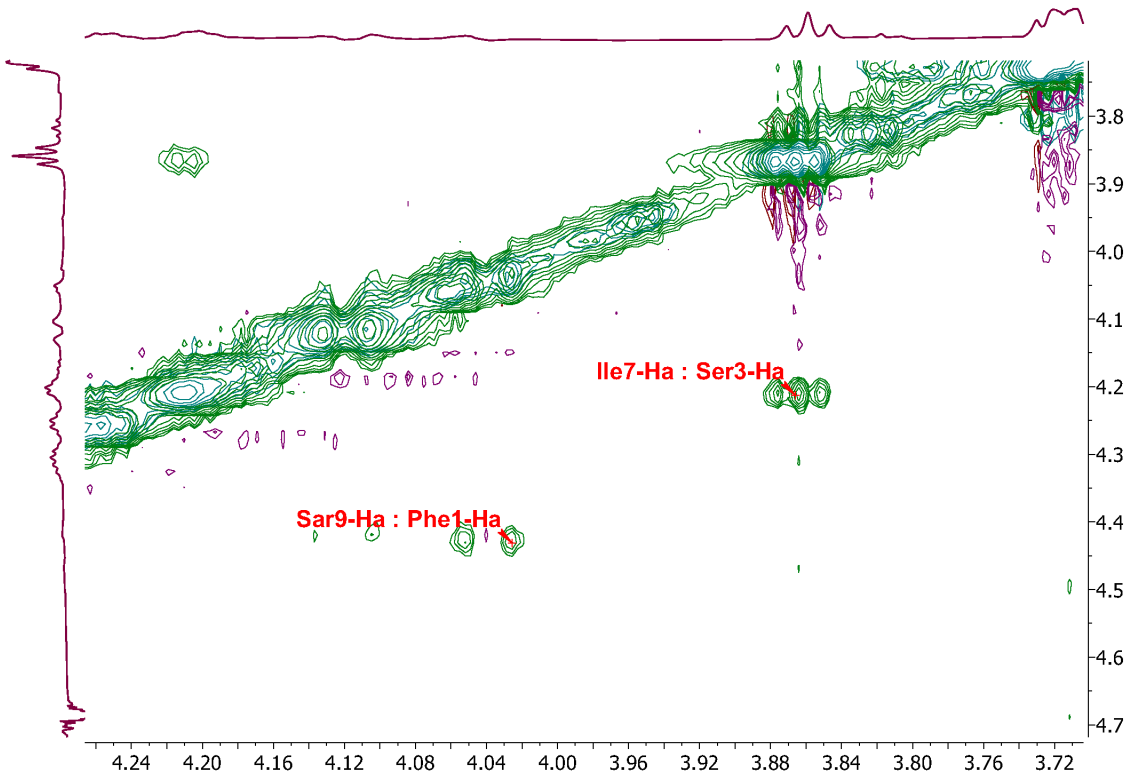

Figure S29. NOESY long-range crosspeaks for **MC4H.** Interactions are evidence for antiparallel of β-strands.

Table S7. Peak assignments for **MC4H**

Residue	αNH	$H_α$	$H_β$	$H_γ$	$H_δ$	$H_ε$	Misc.	$J_{NH - Hα}$
Phe1	8.06	4.42	2.44 2.59	-	6.74 6.89	6.90	$H_ζ$ 6.88	7.86 Hz
His2	8.12	4.31	2.67 2.76	-	6.62	7.90	-	6.40 Hz
Ser3	8.17	4.21	3.40 3.47	-	-	-	-	8.15 Hz
His4	8.45	4.33	2.74 2.86	-	6.82	8.05	-	6.76 Hz
Orn5	-	3.73	1.44	1.22	2.66 3.07	-	δNH 7.94	-
Phe6	8.29	4.48	2.63 2.69	-	6.81	6.80	$H_ζ$ 6.95	6.49 Hz
Ile7	8.16	3.87	1.36	0.69 1.03	0.38	-	γMe 0.44	8.57 Hz
His8	8.36	4.79	2.58 2.79	-	6.83	7.88	-	7.89 Hz
Sar9	-	3.64 4.12	-	-	-	-	αNMe 2.70	-
His10	7.99	4.26	2.71 2.85	-	6.88	8.17	-	6.94 Hz
Orn11	-	3.71	1.46	1.14 1.23	2.99	-	δNH 7.89	-
Trp12	8.04	4.49	2.83	-	6.85	7.15	$H_ζ$ 6.84 $H_η$ 6.62	5.79 Hz

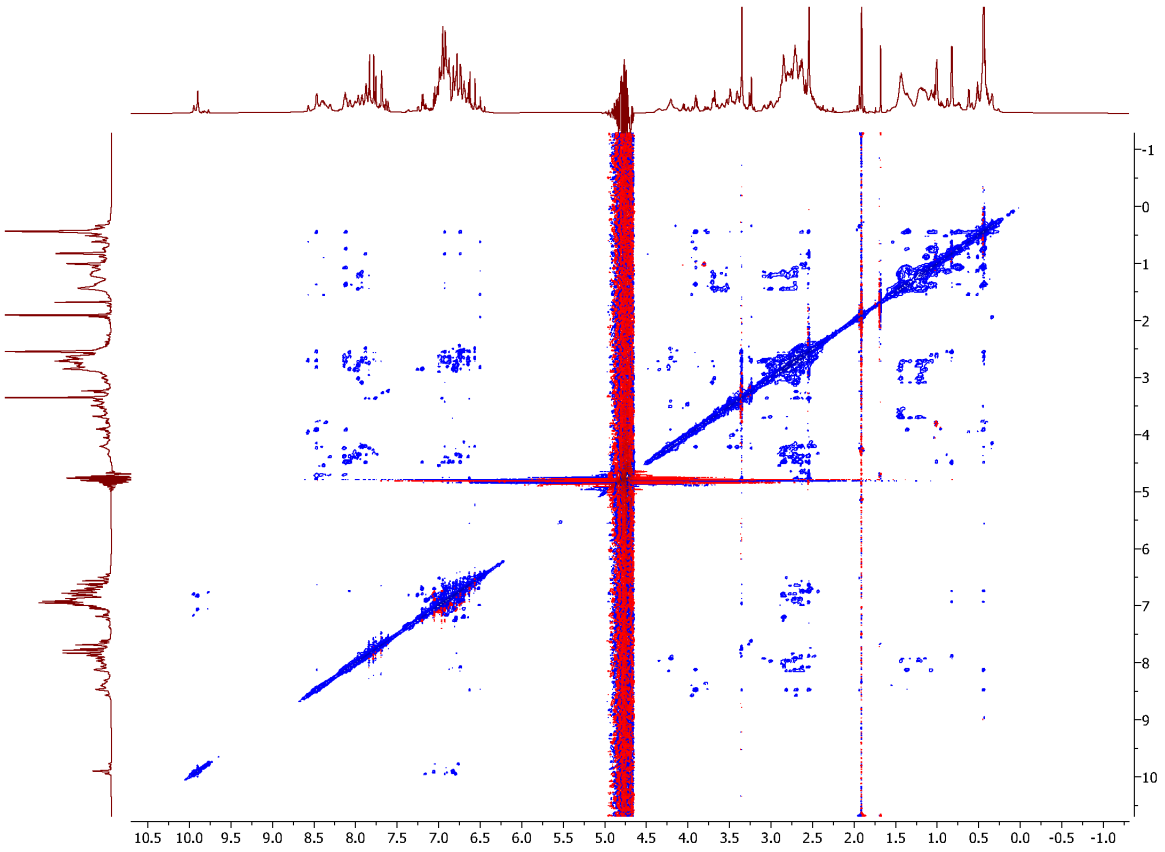

Figure S30. 2D NOESY for **MC4H-MeAMeH**. Sample dissolved in 0.05 M potassium phosphate buffer pH 6.90 with 10% D_2O and 90% H_2O at 280 K.

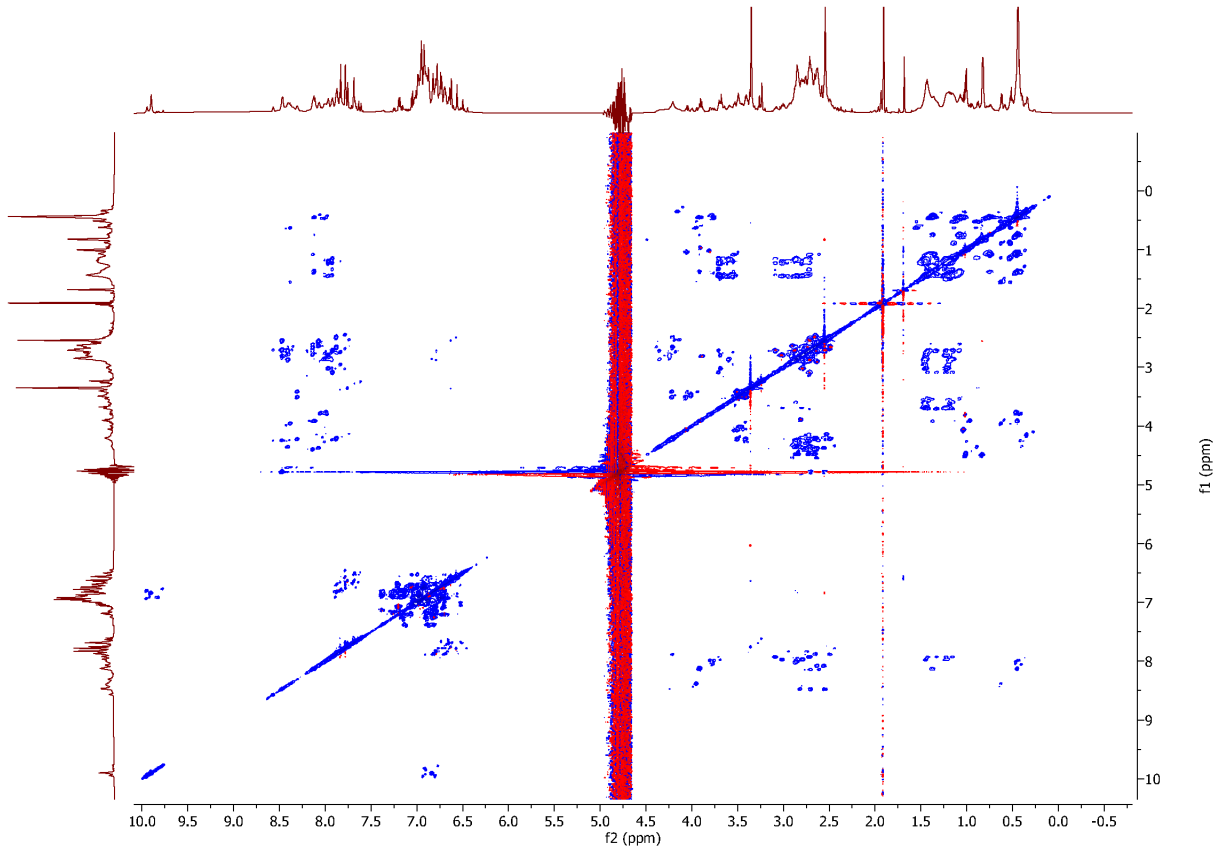

Figure S31. 2D TOCSY for **MC4H-MeAMeH**. Sample dissolved in 0.05 M potassium phosphate buffer pH 6.90 with 10% D_2O and 90% H_2O at 280 K.

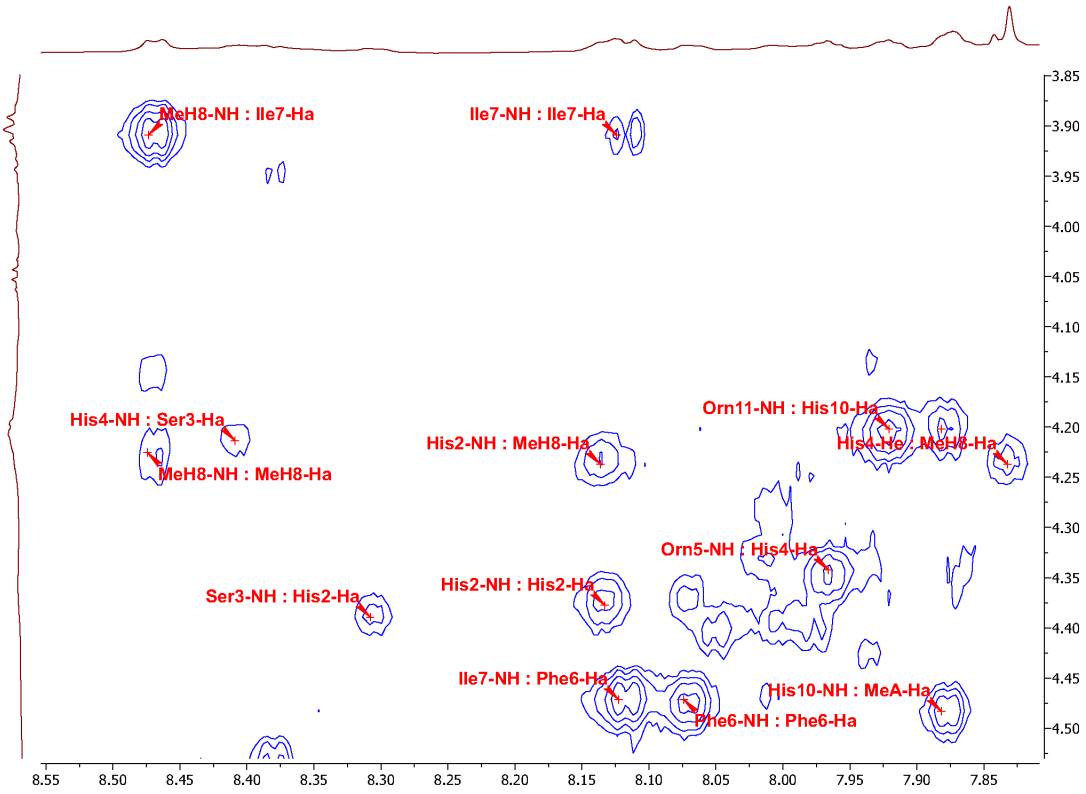

Figure S32. NOESY NH-Hα crosspeaks for **MC4H-MeAMeH**.

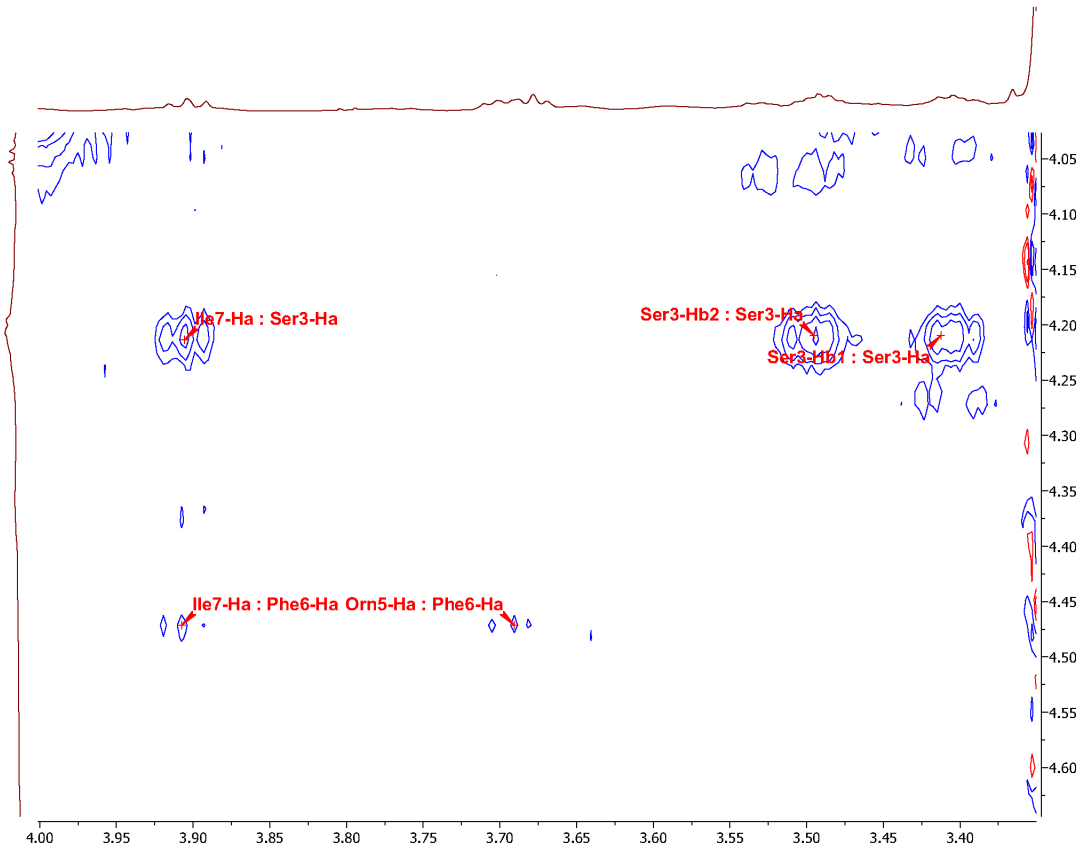

Figure S33. NOESY long-range crosspeaks for **MC4H-MeAMeH**. Interactions are evidence for antiparallel β-strands.

Table S8. Peak assignments for **MC4H-MeAMeH**.

Residue	αNH	H_α	H_β	H_γ	H_δ	H_ε	Misc.	$J_{NH - H\alpha}$
Phe1	8.08	4.46	2.63 2.56	-	6.74	6.92	H_ζ 6.88	7.72 Hz
His2	8.13	4.39	2.60 2.77	-	6.64	7.69	-	8.73 Hz
Ser3	8.31	4.21	3.41 3.50	-	-	-	-	7.35 Hz
His4	8.41	4.34	2.72 2.87	6.78	-	7.83	-	6.72 Hz
Orn5	-	3.69	1.43 1.45	1.20 1.23	2.78 3.01	-	δNH 7.97	-
Phe6	8.07	4.47	2.66 2.73	-	6.83	6.87	H_ζ 6.95	6.16 Hz
Ile7	8.12	3.91	1.37	1.07	0.44	-	γMe 0.73	8.79 Hz
MeH8	8.47	4.24	2.70 2.82	-	6.62	7.76	πNMe 3.36	7.59 Hz
MeA9	-	4.48	0.83	-	-	-	αNMe 2.55	-
His10	7.88	4.20	2.48 2.64	-	6.56	7.78	-	5.22 Hz
Orn11	-	3.70	1.33 1.43	1.15 1.22	2.71 3.08	-	δNH 7.92	-
Trp12	8.01	4.47	2.83 2.86	-	6.83	7.20	H_ζ 6.95 H_η 7.06	-

NMR structure determination and refinement

Before a full CYANA structure could be determined, the library files of the noncanonical residue ornithine (Orn) and its sidechain linkages need to be determined. This was accomplished by first building the residues within MolView and saving them in MOL2 format. The CYANA library file was then generated from the MOL2 files using the CYANA module CYLIB (version 2.2). The Orn side chain needs to be connected through virtual linker atoms and artificial NOEs to define the proper amide bond positioning (**Table S9 and Table S11**). Manually determined distance restraints were used to generate 1000 initial structures annealed for 50,000 steps in CYANA. Lastly, the 100 structures with the lowest target-potentials were selected and further refined within AMBER 14 taking advantage of its full force-field and implicit solvation (see AMBER structure refinement).

Amber structure refinement. Orn atom centered point charges were determined as previously described. In AMBER the method of choice for charge derivation is called the Restrained Electrostatic Potential (RESP) method. The AMBER14 package along with ANTECHAMBER module can be utilized to help in generating all the files needed from the RESP multistage approach. To begin, the MOL2 file of Orn was built within MolView once again. The MOL2 file was read into ANTECHAMBER to generate Gaussian input file for geometry optimization and the HF/6-31G* QM calculation was used to generate the electrostatic potential. Gaussian 16 was used for the previous two steps. Once the ESP data has been determined in Gaussian the multi-conformational RESP stages were automated/executed within ANTECHAMBER. The resulting amber "prepi" file was then utilized within AMBER's "parmchk2" program to generate modified force-field parameters ("frcmod" file). The final input prep ("prepi") file was saved. The 100 CYANA structures were converted into AMBER format using the Leap module and characterized with FF14SB force-field, atomic radii set with mbondi3 and Generalized Born implicit solvation functional form igb=8. All stages of the AMBER refinement were performed with the above settings. AMBER refinement was done in a similar method as previously reported. All the distance and torsional restraints used in CYANA were transferred to AMBER. The CYANA structures were first energy minimized for 10000 steps (5000 steepest descent followed by 5000 conjugate gradient) without experimental restraints. The next phase involving thermal annealing utilized force constants for the NOE distance restraints set to 1 kcal/(mol $Å^2$), torsional set to 540 kcal/(mol rad^2), chirality and trans-omega to 500 kcal/(mol rad^2). A total of three rounds of simulated annealing from 0 to 1000 to 0 Kelvin, regulated by a Berendsen thermostat, were implemented for a total run of 60 ps. The temperature ramping and restraint weighting are the same as previously reported. A standard pairwise Generalized Born solvation (igb=8) was used with no cutoff distance. The time step was set to 1 fs with a total of 60,000 steps. The last step involved a final energy minimization, including NMR restraints and implicit solvation, for 10,000 steps again. The structures from AMBER with the 10 lowest non-restraint energies were kept for structural analysis. Analysis within PROCKECK-NMR shows all the residues to reside in allowed ϕ/ψ space.

Table S9. NOE restraints for MC4H

NH : Hα	Residue	Atom	Residue	Atom	Distance
	Phe1	NH	Trp12	Hα	2.35
	His2	NH	Phe1	Hα	2.70
	Ser3	NH	His2	Hα	3.04
	His4	NH	Ser3	Hα	3.13
	Orn5	NH	His4	Hα	2.60
	Phe6	NH	Orn5	Hα	3.09
	Ile7	NH	Phe6	Hα	2.32
	His8	NH	Ile7	Hα	2.38
	His10	NH	Sar9	αMe2	2.96
	His10	NH	Sar9	αMe3	3.17
	Orn11	NH	His10	Hα	2.53
	Trp12	NH	Orn11	Hα	3.51

NH : NH	Residue	Atom	Residue	Atom	Distance
	His8	NH	Ile7	NH	3.81
	Orn5	NH	His4	NH	4.12

Intra-residue	Residue	Atom	Residue	Atom	Distance
	Phe1	NH	Phe1	Hβ2	2.89
	Phe1	NH	Phe1	Hβ3	3.22
	Phe1	NH	Phe1	Hα	3.13
	His2	NH	His2	Hβ2	3.73
	His2	NH	His2	Hβ3	4.27
	His2	NH	His2	Hα	3.73
	His2	Hα	His2	Hβ2	3.67
	His2	Hα	His2	Hβ3	3.56
	His2	Hδ2	His2	Hβ2	3.67
	His2	Hδ2	His2	Hβ3	4.00
	Ser3	NH	Ser3	Hβ2	4.27
	Ser3	NH	Ser3	Hβ3	3.81
	Ser3	NH	Ser3	Hα	4.27
	Ser3	Hα	Ser3	Hβ2	3.39
	Ser3	Hα	Ser3	Hβ3	3.47
	His4	NH	His4	Hα	3.81
	His4	NH	His4	Hβ2	4.00
	His4	NH	His4	Hβ3	3.61
	His4	Hδ2	His4	Hβ2	3.33
	His4	Hδ2	His4	Hβ3	3.47
	His4	Hδ2	His4	Hα	3.89
	Orn5	δNH	Orn5	Hδ2	2.77
	Orn5	δNH	Orn5	Hδ3	2.97
	Orn5	δNH	Orn5	Hγ	3.04
	Orn5	δNH	Orn5	Hβ	3.43
	Orn5	Hα	Orn5	Hδ	2.91
	Phe6	NH	Phe6	Hβ2	4.27
	Phe6	NH	Phe6	Hβ3	4.80

	Phe6	NH	Phe6	Hα	4.80
	Ile7	NH	Ile7	γMe	3.33
	Ile7	NH	Ile7	Hγ	3.89
	Ile7	NH	Ile7	Hβ	2.73
	Ile7	NH	Ile7	Hα	3.27
	His8	NH	His8	Hβ2	2.93
	His8	NH	His8	Hβ3	3.30
	His8	NH	His8	Hα	3.24
	His8	NH	His8	Hε1	4.00
	His8	Hδ2	His8	Hβ2	3.47
	His8	Hδ2	His8	Hβ3	3.73
	His8	Hδ2	His8	Hα	3.89
	His8	Hα	His8	Hβ2	3.22
	His8	Hα	His8	Hβ3	2.95
	Sar9	αNMe	Sar9	Hα	2.75
	His10	NH	His10	Hβ2	3.33
	His10	NH	His10	Hβ3	3.73
	His10	NH	His10	Hα	3.56
	His10	Hδ2	His10	Hβ2	3.33
	His10	Hδ2	His10	Hβ3	3.89
	Orn11	δNH	Orn11	Hδ2	2.67
	Orn11	δNH	Orn11	Hδ3	2.94
	Orn11	δNH	Orn11	Hγ	2.84
	Orn11	δNH	Orn11	Hβ	4.12
	Orn11	Hα	Orn11	Hδ	2.84
	Trp12	Hε3	Trp12	Hβ	2.71
	Trp12	Hε3	Trp12	Hα	3.39

Inter-residue (short)	**Residue**	**Atom**	**Residue**	**Atom**	**Distance**
	Phe1	NH	Trp12	Hβ	3.11
	His4	NH	Ser3	Hβ	4.12
	Phe6	NH	Orn5	Hβ	4.00
	Ile7	NH	Phe6	Hβ2	3.51
	Ile7	NH	Phe6	Hβ3	3.36
	His8	NH	Ile7	γMe	3.33
	His8	NH	Ile7	Hβ	3.56
	His8	NH	Sar9	αNMe	4.00
	His8	Hα	Sar9	αNMe	2.24

Inter-residue (long)	**Residue**	**Atom**	**Residue**	**Atom**	**Distance**
	Phe1	Hα	Sar	Hα	3.89
	Phe1	Hδ2	Sar	Hα	4.12
	Phe1	Hε2	His10	Hα	3.15
	Ser3	Hα	Ile7	Hα	3.06
	Ile7	δMe	Phe1	Hδ2	3.89
	Ile7	δMe	Phe1	Hε2	4.12
	Ile7	γMe	Phe1	Hδ2	3.27
	Ile7	γMe	Phe1	Hε2	4.12

	Ile7	γMe	Phe1	Hβ	3.33
	His8	NH	Ser3	Hα	4.48
	Orn11	Hγ	Phe1	Hδ2	3.62
	Orn11	Hβ	Phe1	Hε1	3.30
	Trp12	Hε1	His2	Hβ2	5.39
	Trp12	Hε1	His2	Hβ3	4.80

Orn Restraints*	**Residue**	**Atom**	**Residue**	**Atom**	**Distance**
	Orn5	δN	His4	C	1.33
	Orn5	δNH	His4	C	2.00
	Orn5	δC	His4	C	2.43
	Orn5	δN	His4	αC	2.42
	Orn5	δNH	His4	αC	2.53
	Orn5	δN	His4	O	2.25
	Orn5	δNH	His4	O	3.11
	His10	C	Orn11	δN	1.33
	His10	C	Orn11	δNH	2.00
	His10	C	Orn11	δC	2.43
	His10	αC	Orn11	δN	2.42
	His10	αC	Orn11	δNH	2.53
	His10	O	Orn11	δN	2.25
	His10	O	Orn11	δNH	3.11

*Orn restraints were artificially added to ensure proper amide bonding geometry.

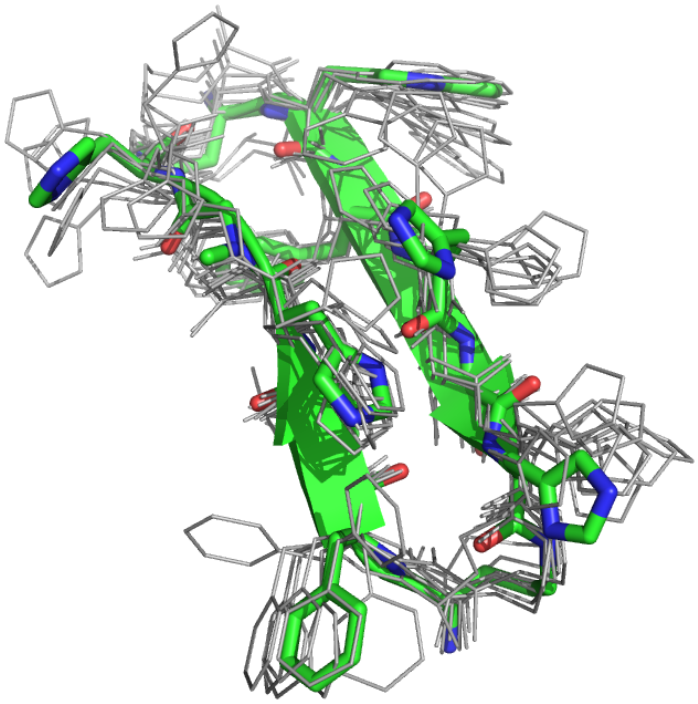

Figure S34. Overlay of 10 lowest energy NMR structures for **MC4H**. The lowest energy structure is shown with ribbon representation.

Table S10. NMR structure and refinement statistics for MC4H

Total Unambiguous Distance Restraints			210
Intra-residue (i,i)			78
Sequential (i, i+1)			50
Medium range ($2 \leq \|i-j\| \leq 4$)			36
Long range ($\|i-j\| > 4$)			46
Intermolecular			0
Total Dihedral Angle Restraints			3
Φ			3
Ψ			0
X1			0
Difference From Mean			
RMSD (Å) (backbone atoms)			0.363
RMSD (Å) (heavy atoms)			0.897
Structure Violation Analysis			
Max dihedral angle violation (°)			0
Max distance violation (Å)			0.23
Mean distance constraint (Å)			0.147 ± 0.034
Mean dihedral angle constraints (°)			0.000 ± 0.000
Energies			
Mean Amber energy (kcal mol^{-1})			36.60
Mean restraint energy (kcal mol^{-1})			2.27
Dihedral Restraints	**Residue**	**Phi (φ)**	**Psi (ψ)**
	Phe1	-160	-70
	Ser3	-60	-40
	Ile7	-160	-70

Table S11. NOE restraints for MC4H-MeAMeH

NH : Hα	Residue	Atom	Residue	Atom	Distance
	Phe1	NH	Trp12	Hα	2.41
	His2	NH	Phe1	Hα	2.68
	Ser3	NH	His2	Hα	3.17
	His4	NH	Ser3	Hα	3.43
	Orn5	NH	His4	Hα	2.50
	Ile7	NH	Phe6	Hα	2.28
	MeH8	NH	Ile7	Hα	2.33
	His10	NH	MeA	Hα	2.64
	Orn11	NH	His10	Hα	2.40

NH : NH	Residue	Atom	Residue	Atom	Distance
	MeH8	NH	Ile7	NH	3.67

Intra-residue	Residue	Atom	Residue	Atom	Distance
	Phe1	NH	Phe1	Hβ2	2.87
	Phe1	NH	Phe1	Hβ3	3.02
	Phe1	NH	Phe1	Hα	3.07
	His2	NH	His2	Hα	2.68
	His2	Hδ2	His2	Hβ2	3.15
	His2	Hδ2	His2	Hβ3	3.36
	His2	Hδ2	His2	Hα	3.47
	Ser3	NH	Ser3	Hβ2	5.39
	Ser3	NH	Ser3	Hβ3	5.39
	Ser3	Hα	Ser3	Hβ2	3.24
	Ser3	Hα	Ser3	Hβ3	3.02
	His4	NH	His4	Hα	4.00
	His4	NH	His4	Hβ2	3.89
	His4	NH	His4	Hβ3	4.27
	His4	Hα	His4	Hβ2	3.47
	His4	Hα	His4	Hβ3	3.27
	His4	Hδ2	His4	Hβ2	3.02
	His4	Hδ2	His4	Hβ3	2.99
	His4	Hδ2	His4	Hα	3.17
	Orn5	Hα	Orn5	Hδ2	3.56
	Orn5	Hα	Orn5	Hδ3	2.95
	Orn5	δNH	Orn5	Hδ2	2.57
	Orn5	δNH	Orn5	Hδ3	2.83
	Ile7	NH	Ile7	Hβ	2.58
	Ile7	NH	Ile7	Hα	3.09
	MeH8	NH	MeH8	Hβ2	3.01
	MeH8	NH	MeH8	Hβ3	2.81
	MeH8	NH	MeH8	Hα	5.39
	MeH8	NH	MeH8	Hδ2	3.73
	MeH8	NH	MeH8	πMe	4.27
	MeH8	Hδ2	MeH8	Hβ2	4.00
	MeH8	Hδ2	MeH8	Hβ3	3.07

	MeH8	Hδ2	MeH8	Hα	4.80
	MeH8	Hδ2	MeH8	πMe	4.27
	MeA9	αNMe	MeA9	Hβ	2.34
	His10	NH	His10	Hβ2	2.96
	His10	NH	His10	Hβ3	3.30
	His10	NH	His10	Hδ2	4.80
	His10	NH	His10	Hα	2.75
	His10	Hα	His10	Hβ2	3.89
	His10	Hα	His10	Hβ3	2.92
	His10	Hδ2	His10	Hβ2	3.89
	His10	Hδ2	His10	Hβ3	3.22
	Orn11	Hα	Orn11	Hδ2	3.67
	Orn11	Hα	Orn11	Hδ3	2.95
	Orn11	δNH	Orn11	Hδ2	2.54
	Orn11	δNH	Orn11	Hδ3	2.91
	Trp12	Hε3	Trp12	Hβ	4.80

Inter-residue (short)	**Residue**	**Atom**	**Residue**	**Atom**	**Distance**
	Phe1	NH	Trp12	Hβ	3.73
	Ile7	NH	Phe6	Hβ2	2.71
	Ile7	NH	Phe6	Hβ3	2.81
	MeH8	NH	Ile7	γMe	4.48
	MeH8	NH	Ile7	Hβ	3.36
	MeH8	NH	Ile7	Hγ12	4.48
	MeH8	NH	Ile7	Hγ23	4.48
	MeH8	Hδ2	Ile7	Hα	4.12
	MeH8	Hα	MeA9	αNMe	4.00
	MeH8	πMe	MeA9	αNMe	2.70

Inter-residue (long)	**Residue**	**Atom**	**Residue**	**Atom**	**Distance**
	Phe1	Hδ2	MeA	Hβ	3.67
	Phe1	Hε2	MeA	Hβ	3.27
	Ile7	Hα	Ser3	Hβ2	4.80
	Ile7	Hα	Ser3	Hβ3	4.48
	Ile7	γMe	Ser3	Hβ2	4.80
	Ile7	γMe	Ser3	Hβ3	5.39
	Ile7	γMe	Phe1	Hβ2	2.76
	Ile7	γMe	Phe1	Hβ3	3.04
	Ile7	δMe	Ser3	Hα	4.00
	Ile7	δMe	Phe1	Hδ2	3.13
	Ile7	δMe	Phe1	Hε2	3.32
	Orn11	Hγ	Phe1	Hε1	4.80
	Orn11	Hβ	Phe1	Hε1	3.81

Orn Restraints*	**Residue**	**Atom**	**Residue**	**Atom**	**Distance**
	Orn5	δN	His4	C	1.33
	Orn5	δNH	His4	C	2.00
	Orn5	δC	His4	C	2.43
	Orn5	δN	His4	αC	2.42

	Orn5	δNH	His4	αC	2.53
	Orn5	δN	His4	O	2.25
	Orn5	δNH	His4	O	3.11
	His10	C	Orn11	δN	1.33
	His10	C	Orn11	δNH	2.00
	His10	C	Orn11	δC	2.43
	His10	αC	Orn11	δN	2.42
	His10	αC	Orn11	δNH	2.53
	His10	O	Orn11	δN	2.25
	His10	O	Orn11	δNH	3.11

*Orn restraints were artificially added to ensure proper amide bonding geometry.

Figure S35. Overlay of 10 lowest energy NMR structures for **MC4H-MeAMeH**. The lowest energy structure is shown with ribbon representation.

Table S12. NMR structure and refinement statistics for MC4H-MeAMeH

Total Unambiguous Distance Restraints			92
Intra-residue (i,i)			56
Sequential (i, i+1)			20
Medium range ($2 \leq \|i-j\| \leq 4$)			8
Long range ($\|i-j\| > 4$)			8
Intermolecular			0
Total Dihedral Angle Restraints			4
Φ			4
Ψ			0
X1			0
Difference From Mean			
RMSD (Å) (backbone atoms)			0.791
RMSD (Å) (heavy atoms)			1.475
Structure Violation Analysis			
Max dihedral angle violation (°)			0
Max distance violation (Å)			0.96
Mean distance constraint (Å)			0.292 ± 0.204
Mean dihedral angle constraints (°)			0.000 ± 0.000
Energies			
Mean Amber energy (kcal mol^{-1})			44.33
Mean restraint energy (kcal mol^{-1})			13.98
Dihedral Restraints	**Residue**	**Phi (φ)**	**Psi (ψ)**
	Phe1	-170	-70
	Ser3	-90	-40
	Phe6	-90	-40
	Ile7	-170	-70

Crystallization

Initial screening for crystallization conditions were performed using 96-well high throughput crystal screen kits purchased from Hampton Research and Molecular Dimensions (Table S13). Optimization of crystals were performed in 24-well plates using the hanging drop method. Optimized conditions used to grow the reported crystals are shown in Table S14.

Sitting drop (96-well)

High-throughput protein crystallization was carried out by a Tecan Freedom Evo 200. Crystallization plates contain 96 wells, with 3 sitting drop compartments per well. 1 µL peptide and 1 µL crystallization were added to each compartment. Assembly of the crystallization plates was temperature controlled, and all completed plates were automatically sealed with an optically clear adhesive. Each screening kit contains 96 unique conditions in 96 deep-well blocks. High-throughput protein crystallization was performed for each peptide using kits shown on Table S13.

Hanging drop (24-well)

24-well hanging drop vapor diffusion crystallization plates with sealing grease were used for bulk crystallization. 500µL of each prepared reagent for bulk crystallization was added into each well. Crystallization reagents were prepared as described in Table S14. A 1 µL drop of sample was added onto a 1 µL reagent drop on a glass cover slide. The cover slide with sample drop was placed over the well and pressed sealed against the sealing grease.

Table S13. High-throughput protein crystallization screening kits.

Manufacturer	Kit	Peptide concentration(s)
Hampton Research	Crystal Screen HT	5 mg/mL, 10 mg/mL
Hampton Research	PEGRx Screen	5 mg/mL, 10 mg/mL
Hampton Research	PEG/Ion Screen	5 mg/mL, 10 mg/mL
Hampton Research	SaltRx Screen	5 mg/mL, 10 mg/mL
Molecular Dimensions	MCSG-1 Screen	5 mg/mL, 10 mg/mL
Molecular Dimensions	MCSG-2 Screen	5 mg/mL, 10 mg/mL
Molecular Dimensions	MCSG-3 Screen	5 mg/mL, 10 mg/mL
Molecular Dimensions	MCSG-4 Screen	5 mg/mL, 10 mg/mL

Table S14. Bulk crystallization conditions for reported peptides.

Peptide	Sample Concentration	Buffer Composition
MC4H	5 mg/mL	0.2 M ammonium sulfate 0.1 M sodium cacodylate trihydrate pH 6.5 30% w/v polyethylene glycol 8000
MC4H-MeH	10 mg/mL	2.0 M sodium formate 0.1 M BIS-TRIS propane pH 7.0

X-ray crystallography

Data were collected at 100 K the Life Sciences Collaborative Access Team beamline 21-ID-D and 21-ID-G at the Advanced Photon Source, Argonne National Laboratory. Diffraction images for each data set were collected using an Eiger 9 detector. Data were processed with *XDS*. **MC4H-MeH** was phased by molecular replacement (with *Phaser*[7]) using an idealized Ala_3 fragment followed by density modification in *ACORN*.[8] *Coot*[9] was used to build the model that were then refined with *Phenix*.[10] **MC4H** was then solved using the structure of **MC4H-MeH** as a model for molecular replacement.

Table S15. SC-XRD data and refinement statistics for crystal structures. Statistics for the highest resolution shell are shown in parentheses.

Sample name	**MC4H**	**MC4H-MeH**
PDB ID	9OXQ	9OXP
Data Collection		
Wavelength (Å)	1.03320	1.03320
Resolution (Å)	23.89 – 1.55	24.92 – 1.25
	(1.605 – 1.55)	(1.295 – 1.25)
Total Observations	88230	94273
	(9012)	(8191)
Unique Observations	13236	7000
	(1323)	(701)
Redundancy	6.7	13.5
	(6.8)	(11.7)
Completeness (%)	98.42	99.19
	(99.77)	(99.86)
I/σ	11.67	49.33
	(2.09)	(8.69)
R_{meas}	0.10520	0.02882
	(0.9224)	(0.2691)
R_{merge}	0.09664	0.02769
	(0.8520)	(0.2573)
Refinement		
$CC_{1/2}$	0.996	1
	(0.752)	(0.981)
R_{free} (%)	0.2571	0.1863
	(0.3281)	(0.2880)
R_{work} (%)	0.2149	0.1635
	(0.2655)	(0.1699)
Avg. B Factor ($Å^2$)	23.57	18.11
RMS Bonds (Å)	0.024	0.007
RMS Angles (°)	1.84	1.47

Table S16. Dihedral angles for **MC4H** from crystallographic data

Chain	Residues	Phi (°)	Psi (°)
A	Phe1	-126.3	144.6
A	His2	-121.1	141.0
A	Ser3	-136.3	137.7
A	His4	-103.5	2.0
A	Phe6	-72.0	154.4
A	Ile7	-115.1	124.8
A	His8	-105.0	149.7
A	Sar9	124.2	151.5
A	His10	-94.9	-33.0
A	Trp12	-110.8	142.4
B	Phe1	-121.2	154.1
B	His2	-139.8	140.1
B	Ser3	-137.4	138.6
B	His4	-93.5	9.5
B	Phe6	-53.4	151.5
B	Ile7	-113.5	120.1
B	His8	-103.7	155.4
B	Sar9	104.3	166.3
B	His10	-137.5	-31.1
B	Trp12	-109.5	141.9
C	Phe1	-128.7	144.4
C	His2	-125.5	151.1
C	Ser3	-146.9	139.3
C	His4	-136.7	25.0
C	Phe6	-65.8	150.5
C	Ile7	-101.0	120.1
C	His8	-94.6	149.4
C	Sar9	117.6	158.8
C	His10	-127.2	18.5
C	Trp12	-85.9	139.5
D	Phe1	-122.2	154.1
D	His2	-143.2	145.6
D	Ser3	-142.3	135.6
D	His4	-110.3	-72.8
D	Phe6	-60.3	143.2
D	Ile7	-105.5	112.1
D	His8	-88.2	152.2
D	Sar9	110.7	173.3
D	His10	-135.2	10.0
D	Trp12	-113.2	139.2
E	Phe1	-133.1	140.2
E	His2	-122.5	145.4
E	Ser3	-158.6	134.7
E	His4	-94.4	16.7
E	Phe6	77.2	154.1
E	Ile7	-105.7	121.2

E	His8	-100.6	148.1
E	Sar9	126.1	137.1
E	His10	-87.0	-14.0
E	Trp12	-102.1	143.2
F	Phe1	-118.2	158.2
F	His2	-139.3	140.4
F	Ser3	-151.1	154.5
F	His4	-140.9	44.5
F	Phe6	-73.0	155.1
F	Ile7	-114.4	114.2
F	His8	-92.3	147.1
F	Sar9	117.6	157.7
F	His10	-124.7	15.3
F	Trp12	-110.4	142.6
G	Phe1	-125.6	142.1
G	His2	-106.5	145.3
G	Ser3	-145.5	151.8
G	His4	-91.1	-34.4
G	Phe6	-71.6	157.7
G	Ile7	-123.3	111.3
G	His8	-98.4	149.7
G	Sar9	120.2	162.5
G	His10	-107.3	12.0
G	Trp12	-105.2	137.9
H	Phe1	-113.5	103.3
H	His2	-122.3	152.6
H	Ser3	-128.2	140.3
H	His4	-83.3	-3.7
H	Phe6	-63.1	153.5
H	Ile7	-140.4	131.5
H	His8	-97.3	160.6
H	Sar9	104.7	167.1
H	His10	-141.9	27.6
H	Trp12	-114.8	140.6

Table S17. Dihedral angles for **MC4H-MeH** from crystallographic data

Chain	Residues	Phi (°)	Psi (°)
A	Phe1	-127.6	147.2
A	His2	-133.7	148.3
A	Ser3	-143.8	151.7
A	His4	-103.5	2.0
A	Phe6	-72.0	154.4
A	Ile7	-116.4	122.5
A	MeH8	-109.1	157.4
A	Sar9	111.1	154.5
A	His10	-94.9	-33.0
A	Trp12	-110.8	142.4
B	Phe1	-107.8	114.6
B	His2	-97.6	155.1
B	Ser3	105.6	163.0
B	His4	-93.5	9.5
B	Phe6	-53.4	151.5
B	Ile7	-107.6	114.8
B	MeH8	-97.1	155.6
B	Sar9	105.0	163.6
B	His10	-137.5	-31.1
B	Trp12	-109.5	141.9

III. References

1 T. L. Hwang and A. J. Shaka, *Journal of Magnetic Resonance, Series A*, 1995, **112**, 275–279.
2 K. Sugase, T. Konuma, J. C. Lansing and P. E. Wright, *J Biomol NMR*, 2013, **56**, 275–283.
3 S. Augé, P.-O. Schmit, C. A. Crutchfield, M. T. Islam, D. J. Harris, E. Durand, M. Clemancey, A.-A. Quoineaud, J.-M. Lancelin, Y. Prigent, F. Taulelle and M.-A. Delsuc, *J. Phys. Chem. B*, 2009, **113**, 1914–1918.
4 V. Thuc Dang, A. Engineer, D. McElheny, A. Drena, J. Telser, K. Tomczak and A. I. Nguyen, *Chemistry – A European Journal*, 2024, **30**, e202402101.
5 S. M. Kelly and N. C. Price, *Curr Protein Pept Sci*, 2000, **1**, 349–384.
6 N. J. Greenfield, *Nat Protoc*, 2006, **1**, 2527–2535.
7 A. J. McCoy, R. W. Grosse-Kunstleve, P. D. Adams, M. D. Winn, L. C. Storoni and R. J. Read, *J Appl Cryst*, 2007, **40**, 658–674.
8 E. J. Dodson and M. M. Woolfson, *Acta Cryst D*, 2009, **65**, 881–891.
9 P. Emsley, B. Lohkamp, W. G. Scott and K. Cowtan, *Acta Cryst D*, 2010, **66**, 486–501.
10 D. Liebschner, P. V. Afonine, M. L. Baker, G. Bunkóczi, V. B. Chen, T. I. Croll, B. Hintze, L.-W. Hung, S. Jain, A. J. McCoy, N. W. Moriarty, R. D. Oeffner, B. K. Poon, M. G. Prisant, R. J. Read, J. S. Richardson, D. C. Richardson, M. D. Sammito, O. V. Sobolev, D. H. Stockwell, T. C. Terwilliger, A. G. Urzhumtsev, L. L. Videau, C. J. Williams and P. D. Adams, *Acta Cryst D*, 2019, **75**, 861–877.